

Low velocity impact response and dynamic stresses of thick high order laminated composite truncated sandwich conical shell based on a new TDOF spring–mass–damper model considering structural damping

A. Azizi¹, S.M.R. Khalili^{*2,3,4} and K. Malekzadeh Fard⁵

¹ Department of Mechanical and Aerospace Engineering, Science and Research Branch, Islamic Azad University, Tehran, Iran

² Faculty of Mechanical Engineering, K.N. Toosi University of Technology, Tehran, Iran

³ Department of Applied Mechanics, Indian Institute of Technology Delhi, New Delhi, 110016, India

⁴ Center of Excellence for Research in Advanced Materials and Structures, Faculty of Mechanical Engineering, K.N. Toosi University of Technology, Pardis Street, Molassadra Avenue, Vanak Square, Tehran, Iran

⁵ Malek Ashtar University of Technology, Department of Mechanical Engineering, 4th Kilometer, Mahsoud RD, Tehran, Iran

(Received April 18, 2017, Revised November 6, 2017, Accepted January 11, 2018)

Abstract. This paper deals with the low velocity impact response and dynamic stresses of composite sandwich truncated conical shells (STCS) with compressible or incompressible core. Impacts are assumed to occur normally over the top face-sheet and the interaction between the impactor and the structure is simulated using a new equivalent three-degree-of-freedom (TDOF) spring-mass-damper (SMD) model. The displacement fields of core and face sheets are considered by higher order and first order shear deformation theory (FSDT), respectively. Considering continuity boundary conditions between the layers, the motion equations are derived based on Hamilton's principal incorporating the curvature, in-plane stress of the core and the structural damping effects based on Kelvin-Voigt model. In order to obtain the contact force, the displacement histories and the dynamic stresses, the differential quadrature method (DQM) is used. The effects of different parameters such as number of the layers of the face sheets, boundary conditions, semi vertex angle of the cone, impact velocity of impactor, trapezoidal shape and in-plane stresses of the core are examined on the low velocity impact response of STCS. Comparison of the present results with those reported by other researchers, confirms the accuracy of the present method. Numerical results show that increasing the impact velocity of the impactor yields to increases in the maximum contact force and deflection, while the contact duration is decreased. In addition, the normal stresses induced in top layer are higher than bottom layer since the top layer is subjected to impact load. Furthermore, with considering structural damping, the contact force and dynamic deflection decreases.

Keywords: low velocity impact; STCS; structural damping; dynamic stresses; higher order theory

1. Introduction

Since thin and thick circular conical shell structures rise to optimum conditions for static and dynamic behavior, they are widely used in mechanical, civil, aerospace, architectural and marine engineering and also various engineering applications such as hoppers, pressure vessels and tanks, space vehicle and spacecrafts, submarines, reactors, jet nozzles. In other words, these structures support applied external forces efficiently by virtue of their geometrical shape (Sofiyev 2011). Although these structures are commonly fabricated from metals, modern sandwich structures are consisted of two thin, stiff metallic or laminated composite face sheets which separated by a relatively thick, light weight inner flexible core (honeycomb or foam) that has energy dissipating property. However, the sandwich structures have widespread usage because of their higher strength/ weight and bending stiffness/ weight ratios of the whole structure without adding much weight (Frostig

and Thomsen 2004). The analytical models and experimental techniques in sandwich plate and shell analysis are found in the works of Allen (2013), Plantema (1966), Zenkert (1995), Vinson (1999) and a comprehensive review with over 800 references on sandwich structures were considered in Noor *et al.* (1996).

The advantages of these structures will be increased where the face sheet is made from the advanced composite laminates (Sun and Wu 1991). Sandwich structures may encounter out-of-plane loads, indentation loads and low-velocity impacts during processing, manufacturing, maintenance or transportation of the composite laminates as in tool drop, bird – strike, runway debris, hail stone, floating debris. When the duration of these impacts is much longer than the period of the lowest natural frequency of the structure, the impact is often termed a low – velocity impact or a large mass impact or a boundary condition controlled impact, as described by Olsson's mass criterion (Anderson 2005).

The main drawback of structural sandwich component is their relatively poor resistance to localized impact loading (Horrigan *et al.* 2000, Abrate 1997, Hiel and Ishai 1992, Nettles and Hodge 1990). Impact resistance of composite

*Corresponding author, Professor,
E-mail: smrkhalili2017@gmail.com

materials is weak because the strain to failure of fiber and the strength of laminate in the thickness – direction are both weak.

Damping can have a very significant effect on dynamic response of structures subjected to impact loads and seismic design requirements for components near or at resonance conditions. There are two main sources of structural damping, i.e., the material damping of the structural members and the damping originated from friction at the joints. If the joints are designed rigid, then the material damping may provide the sole source of structural damping in the system (Sun and Juang 1986). Generally, the damping of metal structures is low, that can induces structure vibrations with high amplitudes. Damping is higher for fiber-reinforced composites and it depends on fiber, resin type, layer orientation, stacking sequence, etc. In sandwich materials, a high part of the energy is dissipated by the transverse shear effects induced in the sandwich core (Assarar *et al.* 2009).

Although extensive research has been devoted to the impact behavior of composite laminates (Abrate 1991, 2005, Sun and Chattopadhyay 1975, Khalili 1992, Mittal 1987, Mittal and Khalili 1994, Wu and Fu-Kuo 1989, Shivakumar *et al.* 1985, Gong *et al.* 1994, Cheng *et al.* 2014), the research on the impact behavior of sandwich structures is somewhat limited (Abrate 2005). Furthermore, most of the researches reported on the impact of composite sandwich structures with experimental or numerical nature (Wang *et al.* 2012, 2013, Leijten *et al.* 2009, Manes *et al.* 2013, Bhuiyan *et al.* 2009, Hassan and Cantwell 2012, Zhang *et al.* 2016). Chai and Zhu (2011) reviewed the numerical mathematical and experimental methods used for the analysis of sandwich panels subjected to impact loading. They analyzed the impact responses according to key parameters and consequently identified various classes of impact. The impact responses on sandwich structures were classified into two main groups, high velocity and low velocity impacts with the focus on the low-velocity impact. According to the mass ratio, the response under low-velocity impact was further subdivided into three possible categories, namely, large, small and medium mass impacts.

The effects of impact parameters such as impact velocity, impact energy, impactor shape and sandwich construction parameters such as core material and thickness and face sheet type on the impact behavior are also considered in many researches. A comprehensive review of analytical models was given by Leijten *et al.* (2009) which classifies the previous researches into three categories: spring – mass models (a combination of global and local springs) used to present the transverse load – formation behavior, energy – balance models that assume a quasi-static behavior of structure and complete models in which the dynamic behavior of the structure is fully modeled. In this context, the work of Ambur and Cruz (1995) may be mentioned in which a local- global analysis was done to determine the contact force and panel displacement.

In driving closed- form solution for the impact response of the composite sandwich panels, the sandwich panels is modeled as a discrete dynamic system with equivalent masses, springs and damper. Shivakumar *et al.* (1985) used

a two- degree-of-freedom model that consisted of four springs for bending, shear, membrane and contact rigidities to predict the impact response of a circular plate. In their model, the contact force and the contact duration for low-velocity impact on circular laminates was calculated. Anderson (2005) performed an investigation of single-degree-of-freedom models for large mass impact on composite sandwich laminates. The stiffness parameters of the models were derived from the results of three-dimensional quasi- static contact analyses of a rigid sphere indenting a multi-layered sandwich laminate. Gong and Lam (2000) used a spring- mass model having two-degrees-of-freedom to determine the history of contact force produced during impact. They also included structural damping in their model. Fatt and Park (2001) presented a simple single-degree-of-freedom spring mass model and obtained the analytic solutions for the transient deformation response of sandwich panels. Zhou and Stronge (2006) presented a contact force correlation for simply support light weight sandwich panel with isotropic face sheets that were obtained by using the principle of minimum potential energy and consideration of local membrane stretching in the impact region. Also, in order to analyze the low-velocity impact on light weight sandwich panel, they used the single and two degree- of- freedom spring- mass models based on quasi- static behavior of the structure. Feli *et al.* (2016) presented an analytical contact force-indentation relationship for clamped circular composite sandwich panels subjected to spherical impactor on a rigid foundation. They considered three parameters for modelling: (1) the core crushing, the rigid perfectly plastic foundation; (2) face sheets based on elastic plate; and (3) local membrane stretching and bending of the face sheets.

Malekzadeh *et al.* (2007) studied a new computational method based on the improved higher order sandwich plate theory (IHSAPT) for face sheets to analyze the transverse low velocity impact on sandwich panels caused by a spherical impactor. In their study, a new three- degree of – freedom (TDOF) springs – masses – damper (SMD) model is proposed to predict the contact force history for composite sandwich panels with transversely flexible core. Khalili *et al.* (2007) presented a new equivalent three-degree-of-freedom (TDOF) spring-masses (SM) model, which accommodated normal impact at any location and used it to predict the low velocity impact response of composite sandwich panels with stiff/flexible core. Their method allowed more than one impactor to act simultaneously on the panel, at different locations, either on the same face sheet or on the opposite sides of the panel. Khalili *et al.* (2014) presented high-order modelling of circular cylindrical composite sandwich shells with a transversely compliant core subjected to low velocity impact. They used energy-balanced model to determine the maximum contact force and then by using a SM model, the contact stiffness corresponding to a linearized contact law was calculated in their study through an iteration process.

The critical time parameters of truncated conical shells with functionally graded coatings and subjected to a time dependent axial load in the large deformation was determined by Sofiyev (2014). The theoretical formulation

was based on the Vonkarman – Donnell – type nonlinear kinematics. The basic equations were reduced to the preposition and Galerkin methods. Nejad *et al.* (2015) utilized a semi-analytical solution for elastic analysis of FGM rotating thick truncated conical shells with axially-varying properties under non-uniform pressure loading based on first-order shear deformation theory and multilayer method. Based on Love's first approximation shell theory, free vibration analysis of conical and cylindrical shells with various boundary conditions was performed by Wilkins *et al.* (1970). In their theory, transverse shear strain was not ignored. Using the finite deformation theory, Tornabene *et al.* (2015) studied the buckling analysis of shallow open conical sandwich shells under uniform external pressure.

Bardell *et al.* (1999) used the h-p finite – element method together with Love's thin shell equations to investigate the natural frequencies of conical sandwich panels having the full range of classical boundary conditions which includes free, clamped, simply supported and shear diaphragm edges.

Tang and Xu (2013) employed Galerkin method for obtaining corresponding nonlinear dynamic response equations for truncated sandwich shallow conical shell based on Reissner's assumption and solved it by Runge-Kutta method. Stability of functionally graded sandwich truncated conical shells reinforced by functionally graded stiffeners and surrounded by an elastic medium and buckling of conical shells under compression was investigated by Dung *et al.* (2016). Morovat (2016) obtained analytical solution for buckling of composite sandwich truncated conical shells subjected to combined external pressure and axial compression load based on the first order deformation theory (FSDT) for face sheets and a 3D elasticity solution of weak core for the flexible core. Malekzadeh Fard and Livani (2015) performed the free vibration analysis of thick truncated conical composite sandwich shells with flexible cores and simply supported boundary conditions based on a new improved and enhanced higher order sandwich shell theory and the first order shear deformation theory for the inner and outer composite face sheets. Bending analysis of sandwich conical shells with flexible cores subjected to concentrated load, uniform distributed load on a patch, harmonic and uniform distributed loads on the top and / or face sheet of the sandwich structure by considering the in-plane hoop stresses of the core was investigated by Malekzadeh Fard (2015). Dey and Karmakar (2014) investigated the effects of delamination on low velocity normal impact response of composite pre-twisted shallow conical shells. The finite element formulation was carried out based on Mindlin's theory for moderate rotational speeds neglecting the Coriolis effect and also the modified Hertzian contact law was utilized to compute the contact force and the time dependent equations were solved by Newmark's time integration algorithm in their study. Bandyopadhyay *et al.* (2016) presented a finite element based method to investigate the hygrothermal effects on the transient dynamic response of delaminated composite pre-twisted conical shells with initial twist impacted at arbitrary locations by multiple spherical impactors.

Due to complexity of the governing equations because of the type of the structure and type of loadings and the related boundary conditions, a highly accurate and fast convergent approximate method such as DQM is essential to use (Tornabene *et al.* 2015, Tornabene and Viola 2009, Setoodeh *et al.* 2012, Malekzadeh and Heydarpour 2013). DQ method is a powerful numerical technique which was originated by Bellman (1970) to solve linear and nonlinear partial differential equations since this method can transform the partial linear and nonlinear equations into a set of algebraic governing equations.

The review of the literature shows that up to now the analytical studies about truncated sandwich conical shells with flexible cores are still very limited. For the first time in the present study, dynamic response analysis of thick laminated STCS with flexible core subjected to low velocity impact under various boundary conditions is performed by using higher order shear deformation theory and DQ method with considering structural damping of the core.

In the Spring mass damper (SMD) model presented in this paper, equivalent stiffness of the impacted top face sheet and the thick laminated truncated conical sandwich shell have been obtained from the static analysis of sandwich panel based on an improved higher order sandwich plate theory. Another important step in the solution of the impact problem is the contact law, which provides the relationship between the impact force and the indentation of the target surface. For isotropic homogeneous linear elastic bodies, the use of the Hertzian contact law is the conventional approach when the indentation is much smaller than the plate thickness. However, for sandwich panels the face sheets are stiff and often anisotropic, while the core is very soft/compliant compared to the face sheets. Accordingly, for sandwich structures the deformation of the core induced by a contact force from a foreign object impact is not small, and the impact energy absorption through indentation is not negligible. However, it is very difficult (if not impossible) to propose a generalized indentation law that would apply to all possible sandwich structures. In the range of low speed impact, the sandwich plate deflection can be approximated as a quasi static process which employs an energy-balance model together with a lumped parameter spring mass model (Foo *et al.* 2008). Therefore a complete model is used to determine the maximum contact force and also the effective contact stiffness corresponding to a nonlinear Hertzian contact law is calculated by using a spring mass damping model.

Spring-mass models are used extensively for analyzing the dynamics of impact. An analytical procedure that includes the transverse flexibility and structural damping of the core of thick laminated truncated conical shells has not yet been dealt with.

In the present paper, the partial differential equations of motion, obtained from Hamilton's concept, are converted into algebraic equations using DQ method. The effects of different parameters such as the core to the face sheet stiffness ratio, the core to the face sheet thickness ratio, semi-vertex angle, large radii of cone-to-length, boundary conditions, in plane stresses of the core, trapezoidal shape of the cross-section, impactor mass, impactor velocity,

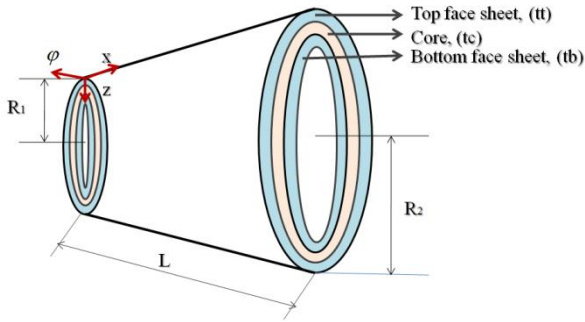


Fig. 1 A schematic figure of laminated STCS

orientation angle of laminas are investigated on the contact force and maximum deflection of thick laminated truncated conical sandwich shells. In addition, the dynamic stresses for the layers are reported.

2. Basic equations

A three-layer laminated STCS is considered as shown in Fig. 1 composed of two orthotropic laminated composite face sheets separated by an orthotropic thick compressible or incompressible core. r_1 , and r_2 indicate the radii of the cone at its small and large ends, respectively, α denotes semi-vertex angle of the cone and L is the cone length along its generator. The thickness of the top face, core and bottom face layers are t^t, t^c, t^b respectively and H is the total thickness of STCS. The origin of the coordinate system (x, φ, z) is located on one corner of the mid plane of the STCS; x is measured along the cone's generator starting at the mid length, φ is the circumferential coordinate and z is a straight line normal to shell mid surface.

Based on Hook's law, the stress-strain relationships for the laminated face sheets may be expressed as (Garg *et al.* 2006)

$$\begin{Bmatrix} \sigma_{xx} \\ \sigma_{\varphi\varphi} \\ \tau_{x\varphi} \\ \tau_{xz} \\ \tau_{\varphi z} \end{Bmatrix}^i = \begin{bmatrix} C_{11} & C_{12} & 0 & 0 & C_{16} \\ C_{21} & C_{22} & 0 & 0 & C_{26} \\ 0 & 0 & C_{44} & C_{45} & 0 \\ 0 & 0 & C_{45} & C_{55} & 0 \\ C_{16} & C_{26} & 0 & 0 & C_{66} \end{bmatrix}^i \begin{Bmatrix} \varepsilon_{xx} \\ \varepsilon_{\varphi\varphi} \\ \gamma_{x\varphi} \\ \gamma_{xz} \\ \gamma_{\varphi z} \end{Bmatrix}^i \quad (1)$$

where C_{mn}^i ($m, n = 1, 2, 6$) are the reduced stiffness coefficients and C_{kl}^i ($k, l = 4, 5$) are the transverse shear stiffness coefficients. The strain-displacement relations for the face sheets can be written based on FSDT as follows (Kheirikhah *et al.* 2012)

$$\varepsilon_{xx}^i = \varepsilon_{0x}^i + z^i \kappa_x^i \quad (2a)$$

$$\varepsilon_{\varphi\varphi}^i = \frac{1}{\left(1 + C_1 \frac{z^i}{R_\varphi}\right)} \left(\varepsilon_{0\varphi}^i + z^i \kappa_\varphi^i\right) \quad (2b)$$

$$\gamma_{x\varphi}^i = \varepsilon_{0x\varphi}^i + z^i \chi_{x\varphi}^i + \frac{1}{\left(1 + C_1 \frac{z^i}{R_\varphi}\right)} \left(\varepsilon_{0\varphi x}^i + z^i \chi_{\varphi x}^i\right) \quad (2c)$$

$$\gamma_{xz}^i = \gamma_{0xz}^i \quad (2d)$$

$$\gamma_{\varphi z}^i = \frac{\gamma_{0\varphi z}^i}{\left(1 + C_1 \frac{z^i}{R_\varphi}\right)} \quad (2e)$$

where

$$\varepsilon_{0x}^i = \frac{\partial u_0^i}{\partial x}, \quad \kappa_x^i = \frac{\partial \theta_x^i}{\partial x} \quad (3a)$$

$$\varepsilon_{0\varphi}^i = \frac{1}{x \sin \alpha} \frac{\partial v_0^i}{\partial \varphi} + \frac{u_0^i}{x} + \frac{w_0^i}{x \tan \alpha}, \quad (3b)$$

$$\kappa_\varphi^i = \frac{1}{x \sin \alpha} \frac{\partial \theta_\varphi^i}{\partial \varphi} + \frac{\theta_x^i}{x}$$

$$\varepsilon_{0x\varphi}^i = \frac{\partial v_0^i}{\partial x}, \quad \varepsilon_{0\varphi x}^i = \frac{1}{x \sin \alpha} \frac{\partial u_0^i}{\partial \varphi} - \frac{v_0^i}{x}, \quad \chi_{x\varphi}^i = \frac{\partial \theta_\varphi^i}{\partial x}, \quad (3c)$$

$$\chi_{\varphi x}^i \frac{1}{x \sin \alpha} \frac{\partial \theta_x^i}{\partial \varphi} - \frac{\theta_\varphi^i}{x} \cdot \gamma_{0x\varphi}^i = \varepsilon_{0x\varphi}^i + \varepsilon_{0\varphi x}^i$$

$$\gamma_{0xz}^i = \frac{\partial w_0^i}{\partial x} + \theta_x^i \quad (3d)$$

$$\gamma_{0\varphi z}^i = \frac{1}{x \sin \alpha} \frac{\partial w_0^i}{\partial \varphi} - \frac{v_0^i}{x \tan \alpha} + \theta_\varphi^i \quad (3e)$$

where u_0^i , v_0^i and w_0^i are the displacements at the mid surface in the α , β and z directions, respectively; θ_x^i and θ_φ^i are rotations of a transverse normal around α and β curvilinear coordinates, respectively. In the above equations i stands for the face sheets, $i = t$ means the top face sheets and $i = b$ means the bottom face sheet.

The stress-strain relationships for the orthotropic core can be read as follows

$$\begin{Bmatrix} \sigma_{xx} \\ \sigma_{\varphi\varphi} \\ \sigma_{zz} \\ \tau_{x\varphi} \\ \tau_{xz} \\ \tau_{\varphi z} \end{Bmatrix}^c = \begin{bmatrix} C_{11} & C_{21} & C_{13} & 0 & 0 & 0 \\ C_{12} & C_{22} & C_{23} & 0 & 0 & 0 \\ C_{13} & C_{23} & C_{33} & 0 & 0 & 0 \\ 0 & 0 & 0 & C_{44} & 0 & 0 \\ 0 & 0 & 0 & 0 & C_{55} & 0 \\ 0 & 0 & 0 & 0 & 0 & C_{66} \end{bmatrix}^c \begin{Bmatrix} \varepsilon_{xx} \\ \varepsilon_{\varphi\varphi} \\ \varepsilon_{zz} \\ \gamma_{x\varphi} \\ \gamma_{xz} \\ \gamma_{\varphi z} \end{Bmatrix}^c \quad (4)$$

where C_{mn}^c ($m, n = 1, \dots, 6$) are the stiffness coefficients of the core. In addition, the strain-displacement relations for the core based on higher order theory can be expressed as

$$\varepsilon_{xx}^c = \varepsilon_{0x}^c + z^c \kappa_x^c + z^{c2} \varepsilon_{0x}^{*c} + z^{c3} \kappa_x^{*c} \quad (5a)$$

$$\varepsilon_{\varphi\varphi}^c = \frac{1}{\left(1 + C_1 \frac{z^c}{R_\varphi}\right)} \left[\varepsilon_{0\varphi}^c + z^c \kappa_\varphi^c + z^{c2} \varepsilon_{0\varphi}^{*c} + z^{c3} \kappa_\varphi^{*c}\right] \quad (5b)$$

$$\varepsilon_{zz}^c = \varepsilon_{0z}^c + z^c \kappa_z^c + z^{c2} \varepsilon_{0z}^{*c} \quad (5c)$$

$$\varepsilon_{x\varphi}^c = \varepsilon_{0x\varphi}^c + z^c \chi_{x\varphi}^c + z^{c2} \varepsilon_{0x\varphi}^{*c} + z^{c3} \chi_{x\varphi}^{*c} \quad (5d)$$

$$\varepsilon_{\varphi x}^c = \frac{1}{\left(1 + C_1 \frac{z^c}{R_\varphi}\right)} \left[\varepsilon_{0\varphi x}^c + z^c \chi_{\varphi x}^c + z^{c2} \varepsilon_{0\varphi x}^{*c} + z^{c3} \chi_{\varphi x}^{*c}\right] \quad (5e)$$

$$\gamma_{xz}^c = [\varepsilon_{0xz}^c + z^c \chi_{xz}^c + z^{c2} \varepsilon_{0xz}^{*c} + z^{c3} \chi_{xz}^{*c}] + [\varepsilon_{0zx}^c + z^c \chi_{zx}^c + z^{c2} \varepsilon_{0zx}^{*c}] \quad (5f)$$

$$\gamma_{\varphi z}^c = \frac{1}{\left(1 + C_1 \frac{z^c}{R_\varphi}\right)} [\varepsilon_{0\varphi z}^c + z^c \chi_{\varphi z}^c + z^{c2} \varepsilon_{0\varphi z}^{*c} + z^{c3} \chi_{\varphi z}^{*c}] + [\varepsilon_{0z\varphi}^c + z^c \chi_{z\varphi}^c + z^{c2} \varepsilon_{0z\varphi}^{*c}] \quad (5g)$$

where

$$\varepsilon_{0x}^c = u_{0,x}^c, \varepsilon_{0\varphi}^c = \frac{1}{x \sin \alpha} v_{0,\varphi}^c + \frac{u_0^c}{x} + \frac{w_0^c}{x \tan \alpha}, \varepsilon_{0z}^c = w_1^c$$

$$\kappa_x^c = u_{1,x}^c, \kappa_\varphi^c = \frac{1}{x \sin \alpha} v_{1,\varphi}^c + \frac{u_1^c}{x} + \frac{w_1^c}{x \tan \alpha}, \kappa_z^c = 2w_2^c \quad (6)$$

$$\varepsilon_{0x}^{*c} = u_{2,x}^c, \varepsilon_{0\varphi}^{*c} = \frac{1}{x \sin \alpha} v_{2,\varphi}^c + \frac{u_2^c}{x} + \frac{w_2^c}{x \tan \alpha}, \varepsilon_{0z}^{*c} = 3w_3^c$$

$$\kappa_x^{*c} = u_{3,x}^c, \kappa_\varphi^{*c} = \frac{1}{x \sin \alpha} v_{3,\varphi}^c + \frac{u_3^c}{x} + \frac{w_3^c}{x \tan \alpha}$$

$$\varepsilon_{0x\varphi}^c = v_{0,x}^c, \varepsilon_{0\varphi x}^c = \frac{1}{x \sin \alpha} u_{0,\varphi}^c - \frac{v_0^c}{x} + \frac{w_0^c}{x \tan \alpha}, \varepsilon_{0xz}^c = w_{0,x}^c$$

$$\chi_{x\varphi}^c = v_{1,x}^c, \chi_{\varphi x}^c = \frac{1}{x \sin \alpha} u_{1,\varphi}^c - \frac{v_1^c}{x} + \frac{w_1^c}{x \tan \alpha}, \chi_{xz}^c = w_{1,x}^c \quad (7)$$

$$\varepsilon_{0x\varphi}^{*c} = v_{2,x}^c, \varepsilon_{0\varphi x}^{*c} = \frac{1}{x \sin \alpha} u_{2,\varphi}^c - \frac{v_2^c}{x} + \frac{w_2^c}{x \tan \alpha}, \varepsilon_{0xz}^{*c} = w_{2,x}^c$$

$$\chi_{x\varphi}^{*c} = v_{3,x}^c, \chi_{\varphi x}^{*c} = \frac{1}{x \sin \alpha} u_{3,\varphi}^c - \frac{v_3^c}{x} + \frac{w_3^c}{x \tan \alpha}, \chi_{xz}^{*c} = w_{3,x}^c$$

$$\varepsilon_{0zx}^c = u_1^c, \varepsilon_{0\varphi z}^c = \frac{1}{x \sin \alpha} w_{0,\varphi}^c - \frac{v_0^c}{x \tan \alpha}, \varepsilon_{0\varphi z}^c = v_1^c$$

$$\chi_{zx}^c = 2u_2^c, \chi_{\varphi z}^c = \frac{1}{x \sin \alpha} w_{1,\varphi}^c - \frac{v_1^c}{x \tan \alpha}, \chi_{\varphi z}^c = 2v_2^c \quad (8)$$

$$\varepsilon_{0zx}^{*c} = 3u_3^c, \varepsilon_{0\varphi z}^{*c} = \frac{1}{x \sin \alpha} w_{2,\varphi}^c - \frac{v_2^c}{x \tan \alpha}, \varepsilon_{0\varphi z}^{*c} = 3v_3^c$$

$$\chi_{\varphi z}^{*c} = \frac{1}{x \sin \alpha} w_{3,\varphi}^c - \frac{v_3^c}{x \tan \alpha}$$

where u_1^c, v_1^c and w_1^c functions are rotational, the parameters $u_2^c, u_3^c, v_2^c, v_3^c, w_2^c$ and w_3^c are the higher-order terms in the Taylor's series expansion.

Reminding that there is no slipping between the face sheets and the core, the following relations are written (Kheirikhah *et al.* 2012)

$$\begin{cases} u^c|_{z=\frac{t^c}{2}} = u^t|_{z=\frac{t^c}{2}} \\ u^c|_{z=-\frac{t^c}{2}} = u^b|_{z=-\frac{t^c}{2}} \end{cases}, \begin{cases} v^c|_{z=\frac{t^c}{2}} = v^t|_{z=\frac{t^c}{2}} \\ v^c|_{z=-\frac{t^c}{2}} = v^b|_{z=-\frac{t^c}{2}} \end{cases}, \begin{cases} w^c|_{z=\frac{t^c}{2}} = w^t|_{z=\frac{t^c}{2}} \\ w^c|_{z=-\frac{t^c}{2}} = w^b|_{z=-\frac{t^c}{2}} \end{cases} \quad (9)$$

3. Governing equations

In order to derive the motion equations of laminated STCS, the energy method is used. The first variation of the strain energy for STCS during the elastic deformation is

$$\int_{t_1}^{t_2} \delta U^c dt + \sum_i^{t,b} \int_{t_1}^{t_2} \delta U^i dt$$

$$= \int_0^t \int_z \int_A \left(h_x \sigma_x^c \delta \varepsilon_x^c + h_\varphi \sigma_\varphi^c \delta \varepsilon_\varphi^c + \sigma_z^c \delta \varepsilon_z^c + h_{x\varphi} \tau_{x\varphi}^c \delta \gamma_{x\varphi}^c + \tau_{x\varphi}^c \delta \gamma_{x\varphi}^c + \tau_{\varphi z}^c \delta \gamma_{\varphi z}^c \right) dA^c dz dt \quad (10)$$

$$+ \sum_i^{t,b} \left\{ \int_0^t \int_{z^i} \int_A \left(\sigma_x^i \delta \varepsilon_x^i + \sigma_\varphi^i \delta \varepsilon_\varphi^i + \tau_{x\varphi}^i \delta \gamma_{x\varphi}^i + \tau_{xz}^i \delta \gamma_{xz}^i + \tau_{\varphi z}^i \delta \gamma_{\varphi z}^i \right) dA^i dz^i dt \right\}$$

The kinetic energy for STCS is given by

$$E = \frac{1}{2} \sum_i^{t,b,c} \int_{V^i} \rho^i (\dot{u}^i{}^2 + \dot{v}^i{}^2 + \dot{w}^i{}^2) dV^i \quad (11)$$

where ρ^i ($i = t, b, c$) is the mass per unit volume of the top and the bottom face sheets and the core respectively; $\dot{u}^i, \dot{v}^i, \dot{w}^i$ ($i = t, b, c$) are the velocities in the x, φ and z directions, respectively; “.” denotes the first time derivative; V^i ($i = t, b, c$) is the volume of the top and the bottom face sheets and the core, respectively. The first variation of the kinetic energy can be written as

$$\int_0^t \delta E dt = \sum_i^{t,b} \int_0^t \delta E^i dt + \int_0^t \delta E^c dt$$

$$= \sum_i^{t,b} \left\{ - \int_0^t \int_A [(I_0^i \ddot{u}_0^i + I_1^i \ddot{\theta}_x^i) \delta u_0^i + (I_1^i \dot{u}_0^i + I_2^i \dot{\theta}_x^i) \delta \theta_x^i + (I_0^i \dot{v}_0^i + I_1^i \dot{\theta}_\varphi^i) \delta v_0^i + (I_1^i \dot{u}_0^i + I_2^i \dot{\theta}_\varphi^i) \delta \theta_\varphi^i + (I_0^i \dot{w}^i) \delta w^i] (x \sin \alpha dx d\varphi) dt \right\}$$

$$- \int_0^t \int_A [(I_0^c \ddot{u}_0^c + I_1^c \ddot{u}_1^c + I_2^c \ddot{u}_2^c + I_3^c \ddot{u}_3^c) \delta u_0^c + (I_1^c \dot{u}_0^c + I_2^c \dot{u}_1^c + I_3^c \dot{u}_2^c + I_4^c \dot{u}_3^c) \delta u_1^c + (I_2^c \dot{u}_0^c + I_3^c \dot{u}_1^c + I_4^c \dot{u}_2^c + I_5^c \dot{u}_3^c) \delta u_2^c + (I_3^c \dot{u}_0^c + I_4^c \dot{u}_1^c + I_5^c \dot{u}_2^c + I_6^c \dot{u}_3^c) \delta u_3^c + (I_0^c \dot{v}_0^c + I_1^c \dot{v}_1^c + I_2^c \dot{v}_2^c + I_3^c \dot{v}_3^c) \delta v_0^c + (I_1^c \dot{v}_0^c + I_2^c \dot{v}_1^c + I_3^c \dot{v}_2^c + I_4^c \dot{v}_3^c) \delta v_1^c + (I_2^c \dot{v}_0^c + I_3^c \dot{v}_1^c + I_4^c \dot{v}_2^c + I_5^c \dot{v}_3^c) \delta v_2^c + (I_3^c \dot{v}_0^c + I_4^c \dot{v}_1^c + I_5^c \dot{v}_2^c + I_6^c \dot{v}_3^c) \delta v_3^c + (I_0^c \dot{w}_0^c + I_1^c \dot{w}_1^c + I_2^c \dot{w}_2^c + I_3^c \dot{w}_3^c) \delta w_0^c + (I_1^c \dot{w}_0^c + I_2^c \dot{w}_1^c + I_3^c \dot{w}_2^c + I_4^c \dot{w}_3^c) \delta w_1^c + (I_2^c \dot{w}_0^c + I_3^c \dot{w}_1^c + I_4^c \dot{w}_2^c + I_5^c \dot{w}_3^c) \delta w_2^c + (I_3^c \dot{w}_0^c + I_4^c \dot{w}_1^c + I_5^c \dot{w}_2^c + I_6^c \dot{w}_3^c) \delta w_3^c] (x \sin \alpha dx d\varphi) dt \quad (12)$$

where

$$I_n^i = \int_z \rho^i \left(1 + C_1 \frac{z^i}{R_\varphi} \right) (z^n) dz, \quad i = t, b, c \quad \text{and} \quad n = 1 \text{ to } 6 \quad (13)$$

However, substituting Eqs. (10) and (12) into following equation

$$\delta \int_{t_1}^{t_2} (L) dt = \delta \int_{t_1}^{t_2} [E - (U + W)] dt = 0 \quad (14)$$

integrating by parts and collecting the coefficients of independent variations in $\delta u_0^b, \delta v_0^t, \delta w^t, \delta \theta_x^t, \delta \theta_\phi^t, \delta u_2^c, \delta v_2^c, \delta w_2^c, \delta u_3^c, \delta v_3^c, \delta w_3^c, \delta u_0^b, \delta v_0^b, \delta w^b, \delta \theta_x^b, \delta \theta_\phi^b$, six sixteen equations of motion for STCS may be expressed as

$$\begin{aligned} & \left(\frac{h_x}{2x} \right) \{N_x^c\} + \left(\frac{h_x}{2} \right) \{N_{x,x}^c\} + \left(\frac{h_x}{t^c x} \right) \{M_x^c\} + \left(\frac{h_x}{t^c} \right) \{M_{x,x}^c\} \\ & - \left(\frac{h_\phi}{2x} \right) \{N_\phi^c\} - \left(\frac{h_\phi}{t^c x} \right) \{M_\phi^c\} + \left(\frac{h_{x\phi}}{2x \sin \alpha} \right) \{N_{\phi x}^c\} \\ & + \left(\frac{h_{x\phi}}{t^c x \sin \alpha} \right) \{M_{\phi x}^c\} - \left(\frac{1}{t^c} \right) \{Q_{zx}^c\} + \left(\frac{1}{x} \right) \{N_x^t\} \\ & + \{N_{x,x}^t\} - \left(\frac{1}{x} \right) \{N_\phi^t\} + \left(\frac{1}{x \sin \alpha} \right) \{N_{\phi x}^t\} \\ & = \left[\left(\frac{1}{4} I_0^c + \frac{1}{t^c} I_1^c + \frac{1}{t^{c2}} I_2^c \right) + I_0^t \right] \ddot{u}_0^t \\ & + \left[\left(-\frac{t^t}{8} I_0^c - \frac{t^t}{2t^c} I_1^c - \frac{t^t}{2t^{c2}} I_2^c \right) + I_1^t \right] \ddot{\theta}_x^t + \end{aligned} \quad (15a)$$

$$\begin{aligned} & \left[-\frac{t^{c2}}{8} I_0^c - \frac{t^c}{4} I_1^c + \frac{1}{2} I_2^c + \frac{1}{t^c} I_3^c \right] \ddot{u}_2^c \\ & + \left[-\frac{t^{c2}}{8} I_1^c - \frac{t^c}{4} I_2^c + \frac{1}{2} I_3^c + \frac{1}{t^c} I_4^c \right] \ddot{u}_3^c \\ & + \left[\frac{1}{4} I_0^c - \frac{1}{t^{c2}} I_2^c \right] \ddot{u}_0^b + \left[\frac{t^b}{8} I_0^c - \frac{t^b}{2t^{c2}} I_2^c \right] \ddot{\theta}_x^b \end{aligned}$$

$$\begin{aligned} & \left(\frac{h_\phi}{2x \sin \alpha} \right) \{N_{\phi,\phi}^c\} + \left(\frac{h_\phi}{t^c x \sin \alpha} \right) \{M_{\phi,\phi}^c\} + \left(\frac{h_{x\phi}}{2x} \right) \{N_{x\phi}^c\} \\ & + \left(\frac{h_{x\phi}}{2} \right) \{N_{x\phi,x}^c\} + \left(\frac{h_{x\phi}}{2x} \right) \{N_{\phi x}^c\} + \left(\frac{h_{x\phi}}{t^c x} \right) \{M_{x\phi}^c\} \\ & + \left(\frac{h_{x\phi}}{t^c} \right) \{M_{x\phi,x}^c\} + \left(\frac{h_{x\phi}}{t^c x} \right) \{M_{\phi x}^c\} + \left(\frac{1}{2x \tan \alpha} \right) \{Q_{\phi z}^c\} \\ & + \left(\frac{1}{t^c x \tan \alpha} \right) \{S_{\phi z}^c\} - \left(\frac{1}{t^c} \right) \{Q_{z\phi}^c\} + \left(\frac{1}{x \sin \alpha} \right) \{N_{\phi,\phi}^t\} \\ & + \left(\frac{1}{x} \right) \{N_{x\phi}^t\} + \{N_{x\phi,x}^t\} + \left(\frac{1}{x} \right) \{N_{\phi x}^t\} + \left(\frac{k_s}{x \tan \alpha} \right) \{Q_{\phi z}^t\} = \\ & \left[\left(\frac{1}{4} I_0^c + \frac{1}{t^c} I_1^c + \frac{1}{t^{c2}} I_2^c \right) + I_0^t \right] \ddot{v}_0^t \end{aligned} \quad (15b)$$

$$\begin{aligned} & + \left[\left(-\frac{t^t}{8} I_0^c - \frac{t^t}{2t^c} I_1^c - \frac{t^t}{2t^{c2}} I_2^c \right) + I_1^t \right] \ddot{\theta}_\phi^t + \\ & \left[-\frac{t^{c2}}{8} I_0^c - \frac{t^c}{4} I_1^c + \frac{1}{2} I_2^c + \frac{1}{t^c} I_3^c \right] \ddot{v}_2^c \\ & + \left[-\frac{t^{c2}}{8} I_1^c - \frac{t^c}{4} I_2^c + \frac{1}{2} I_3^c + \frac{1}{t^c} I_4^c \right] \ddot{v}_3^c \\ & + \left[\frac{1}{4} I_0^c - \frac{1}{t^{c2}} I_2^c \right] \ddot{v}_0^b + \left[\frac{t^b}{8} I_0^c - \frac{t^b}{2t^{c2}} I_2^c \right] \ddot{\theta}_\phi^b \end{aligned}$$

$$\begin{aligned} & - \left(\frac{h_\phi}{2x \tan \phi} \right) \{N_\phi^c\} - \left(\frac{h_\phi}{t^c x \tan \phi} \right) \{M_\phi^c\} - \left(\frac{1}{t^c} \right) \{N_z^c\} \\ & + \left(\frac{1}{2x} \right) \{Q_{xz}^c\} + \left(\frac{1}{2} \right) \{Q_{xz,x}^c\} + \left(\frac{1}{xt^c} \right) \{S_{xz}^c\} + \left(\frac{1}{t^c} \right) \{S_{xz,x}^c\} \\ & + \left(\frac{1}{2x \sin \phi} \right) \{Q_{\phi z}^c\} + \left(\frac{1}{x \sin \phi} \right) \{S_{\phi z}^c\} - \left(\frac{1}{x \sin \phi} \right) \{N_\phi^t\} \\ & + \left(\frac{k_s}{x} \right) \{Q_{xz}^t\} + k_s \{Q_{xz,x}^t\} + \left(\frac{k_s}{x \sin \phi} \right) \{Q_{\phi z}^t\} \end{aligned} \quad (15c)$$

$$\begin{aligned} & = \left[\left(\frac{1}{4} I_0^c + \frac{1}{t^c} I_1^c + \frac{1}{t^{c2}} I_2^c \right) + I_0^t \right] \ddot{w}^t \\ & + \left[-\frac{t^{c2}}{8} I_0^c - \frac{t^c}{4} I_1^c + \frac{1}{2} I_2^c + \frac{1}{t^c} I_3^c \right] \ddot{w}_2^c + \\ & \left[-\frac{t^{c2}}{8} I_1^c - \frac{t^c}{4} I_2^c + \frac{1}{2} I_3^c + \frac{1}{t^c} I_4^c \right] \ddot{w}_3^c + \left[\frac{1}{4} I_0^c - \frac{1}{t^{c2}} I_2^c \right] \ddot{w}^b \\ & - \left(\frac{h_x t^t}{4x} \right) \{N_x^c\} - \left(\frac{h_x t^t}{4} \right) \{N_{x,x}^c\} - \left(\frac{h_x t^t}{2xt^c} \right) \{M_x^c\} \\ & - \left(\frac{h_x t^t}{2t^c} \right) \{M_{x,x}^c\} + \left(\frac{h_\phi t^t}{4x} \right) \{N_\phi^c\} + \left(\frac{h_\phi t^t}{2xt^c} \right) \{M_\phi^c\} - \\ & \left(\frac{h_{x\phi} t^t}{4x \sin \alpha} \right) \{N_{\phi x}^c\} - \left(\frac{h_{x\phi} t^t}{2x \sin \alpha t^c} \right) \{M_{\phi x}^c\} \\ & + \left(\frac{t^t}{2t^c} \right) \{Q_{zx}^c\} + \left(\frac{1}{x} \right) \{M_x^t\} + \{M_{x,x}^t\} - \left(\frac{1}{x} \right) \{M_\phi^t\} + \\ & \left(\frac{1}{x \sin \alpha} \right) \{M_{\phi x}^t\} - k_s \{Q_{zx}^t\} = \end{aligned} \quad (15d)$$

$$\begin{aligned} & \left[\left(-\frac{t^t}{8} I_0^c - \frac{t^t}{2t^c} I_1^c - \frac{t^t}{2t^{c2}} I_2^c \right) + I_1^t \right] \ddot{u}_0^t + \\ & \left[\left(\frac{t^{t2}}{16} I_0^c + \frac{t^{t2}}{4t^c} I_1^c + \frac{t^{t2} I_2^c}{4t^{c2}} \right) + I_2^t \right] \ddot{\theta}_x^t \\ & + \left[\frac{t^t t^{c2}}{16} I_0^c + \frac{t^t t^c}{8} I_1^c - \frac{t^t}{4} I_2^c - \frac{t^t}{2t^c} I_3^c \right] \ddot{u}_2^c + \\ & \left[\frac{t^t t^{c2}}{16} I_1^c + \frac{t^t t^c}{8} I_2^c - \frac{t^t}{4} I_3^c - \frac{t^t}{2t^c} I_4^c \right] \ddot{u}_3^c \\ & + \left[-\frac{t^t}{8} I_0^c + \frac{t^t}{2t^{c2}} I_2^c \right] \ddot{u}_0^b + \left[-\frac{t^t t^b}{16} I_0^c + \frac{t^t t^b}{4t^{c2}} I_2^c \right] \ddot{\theta}_x^b \end{aligned}$$

$$\begin{aligned} & - \left(\frac{h_\phi t^t}{4x \sin \phi} \right) \{N_{\phi,\phi}^c\} - \left(\frac{h_\phi t^t}{2x \sin \phi t^c} \right) \{M_{\phi,\phi}^c\} - \left(\frac{h_{x\phi} t^t}{4x} \right) \{N_{x\phi}^c\} \\ & - \left(\frac{h_{x\phi} t^t}{4x} \right) \{N_{x\phi,x}^c\} - \left(\frac{h_{x\phi} t^t}{4} \right) \{N_{\phi x}^c\} - \left(\frac{h_{x\phi} t^t}{2xt^c} \right) \{M_{\phi x}^c\} \\ & - \left(\frac{h_{x\phi} t^t}{2xt^c} \right) \{M_{x\phi}^c\} - \left(\frac{h_{x\phi} t^t}{t^c} \right) \{M_{x\phi,x}^c\} - \left(\frac{t^t}{4x \tan \phi} \right) \{Q_{\phi z}^c\} \\ & - \left(\frac{t^t}{2t^c x \tan \phi} \right) \{S_{\phi z}^c\} + \left(\frac{t^t}{2t^c} \right) \{Q_{z\phi}^c\} + \left(\frac{1}{x \sin \phi} \right) \{M_{\phi,\phi}^t\} \\ & + \left(\frac{1}{x} \right) \{M_{\phi x}^t\} + \left(\frac{1}{x} \right) \{M_{x\phi}^t\} + \{M_{x\phi,x}^t\} + \left(\frac{k_s}{x \tan \phi} \right) \{S_{\phi z}^t\} - \\ & k_s \{Q_{z\phi}^t\} = \left[\left(-\frac{t^t}{8} I_0^c - \frac{t^t}{2t^c} I_1^c - \frac{t^t}{2t^{c2}} I_2^c \right) + I_1^t \right] \ddot{v}_0^t \end{aligned} \quad (15e)$$

$$\begin{aligned}
 & + \left[\left(\frac{t'^2}{16} I_0^c + \frac{t'^2}{4t^c} I_1^c + \frac{t'^2 I_2^c}{4t'^2} \right) + I_2^t \right] \theta_\varphi^- + \\
 & \left[\frac{t' t'^2}{16} I_0^c + \frac{t' t'^c}{8} I_1^c - \frac{t'}{4} I_2^c - \frac{t'}{2t^c} I_3^c \right] v_2^c \\
 & + \left[\frac{t' t'^2}{16} I_1^c + \frac{t' t'^c}{8} I_2^c - \frac{t'}{4} I_3^c - \frac{t'}{2t^c} I_4^c \right] v_3^c \\
 & + \left[-\frac{t'}{8} I_0^c + \frac{t'}{2t^c} I_2^c \right] v_0^b + \left[-\frac{t' t'^b}{16} I_0^c + \frac{t' t'^b}{4t^c} I_2^c \right] \theta_\varphi^b
 \end{aligned} \tag{15e}$$

$$\begin{aligned}
 & - \left(\frac{h_x t'^{c2}}{4x} \right) \{N_x^c\} - \left(\frac{h_x t'^{c2}}{4} \right) \{N_{x,x}^c\} + \left(\frac{h_x}{x} \right) \{N_x^{*c}\} \\
 & + h_x \{N_{x,x}^{*c}\} + \left(\frac{h_\varphi t'^{c2}}{4x} \right) \{N_\varphi^c\} - \left(\frac{h_\varphi}{x} \right) \{N_\varphi^{*c}\} - \\
 & \left(\frac{h_x \varphi t'^{c2}}{4x \sin \varphi} \right) \{N_{\varphi x, \varphi}^c\} + \left(\frac{h_x \varphi}{x \sin \varphi} \right) \{N_{\varphi x, \varphi}^{*c}\} - 2 \{S_{zx}^c\} \\
 & = \left[-\frac{t'^2}{8} I_0^c - \frac{t^c}{4} I_1^c + \frac{1}{2} I_2^c + \frac{1}{t^c} I_3^c \right] \ddot{u}_0^t + \\
 & \left[\frac{t'^2 t'}{16} I_0^c + \frac{t' t'^c}{8} I_1^c - \frac{t'}{4} I_2^c - \frac{t'}{2t^c} I_3^c \right] \ddot{\theta}_x^t \\
 & + \left[\frac{t'^4}{16} I_0^c - \frac{t'^2}{2} I_2^c + I_4^c \right] \ddot{u}_2^c + \left[\frac{t'^4}{16} I_1^c - \frac{t'^2}{2} I_3^c + I_5^c \right] \ddot{u}_3^c \\
 & + \left[-\frac{t'^2}{8} I_0^c + \frac{t^c}{4} I_1^c + \frac{1}{2} I_2^c - \frac{1}{t^c} I_3^c \right] \ddot{u}_0^b \\
 & + \left[-\frac{t'^2 t^b}{16} I_0^c + \frac{t^c t^b}{8} I_1^c + \frac{t^b}{4} I_2^c - \frac{t^b}{2t^c} I_3^c \right] \ddot{\theta}_x^b
 \end{aligned} \tag{15f}$$

$$\begin{aligned}
 & - \left(\frac{h_\varphi t'^{c2}}{4x \sin \alpha} \right) \{N_{\varphi, \varphi}^c\} + \left(\frac{h_\varphi}{x \sin \alpha} \right) \{N_{\varphi, \varphi}^{*c}\} - \left(\frac{h_x \varphi t'^{c2}}{4x} \right) \{N_{\varphi x}^c\} \\
 & - \left(\frac{h_x \varphi t'^{c2}}{4x} \right) \{N_{x\varphi}^c\} - \left(\frac{h_x \varphi t'^{c2}}{4} \right) \{N_{x\varphi, x}^c\} + \left(\frac{h_x \varphi}{x} \right) \{N_{\varphi x}^{*c}\} \\
 & + \left(\frac{h_x \varphi}{x} \right) \{N_{x\varphi}^{*c}\} + h_x \varphi \{N_{x\varphi, x}^{*c}\} - \left(\frac{t'^2}{4x \tan \alpha} \right) \{Q_{\varphi z}^c\} \\
 & + \left(\frac{1}{x \tan \alpha} \right) \{Q_{\varphi z}^{*c}\} - 2 \{S_{z\varphi}^c\} = \\
 & \left[-\frac{t'^2}{8} I_0^c - \frac{t^c}{4} I_1^c + \frac{1}{2} I_2^c + \frac{1}{t^c} I_3^c \right] \dot{v}_0^t \\
 & + \left[\frac{t'^2 t'}{16} I_0^c + \frac{t' t'^c}{8} I_1^c - \frac{t'}{4} I_2^c - \frac{t'}{2t^c} I_3^c \right] \ddot{\theta}_\varphi^t \\
 & + \left[\frac{t'^4}{16} I_0^c - \frac{t'^2}{2} I_2^c + I_4^c \right] \dot{v}_2^c + \left[\frac{t'^4}{16} I_1^c - \frac{t'^2}{2} I_3^c + I_5^c \right] \dot{v}_3^c \\
 & + \left[-\frac{t'^2}{8} I_0^c + \frac{t^c}{4} I_1^c + \frac{1}{2} I_2^c - \frac{1}{t^c} I_3^c \right] \dot{v}_0^b \\
 & + \left[-\frac{t'^2 t^b}{16} I_0^c + \frac{t^c t^b}{8} I_1^c + \frac{t^b}{4} I_2^c - \frac{t^b}{2t^c} I_3^c \right] \ddot{\theta}_\varphi^b
 \end{aligned} \tag{15g}$$

$$\begin{aligned}
 & \left(\frac{h_\varphi t'^{c2}}{4x \tan \alpha} \right) \{N_\varphi^c\} - \left(\frac{h_\varphi}{x \tan \alpha} \right) \{N_\varphi^{*c}\} - 2 \{M_z^c\} - \\
 & \left(\frac{t'^2}{4x} \right) \{Q_{xz}^c\} - \left(\frac{t'^2}{4} \right) \{Q_{xz, x}^c\} + \left(\frac{1}{x} \right) \{Q_{xz}^{*c}\} + \\
 & \{Q_{xz, x}^{*c}\} - \left(\frac{t'^2}{4x \sin \alpha} \right) \{Q_{\varphi z, \varphi}^c\} + \left(\frac{1}{x \sin \alpha} \right) \{Q_{\varphi z, \varphi}^{*c}\}
 \end{aligned} \tag{15h}$$

$$\begin{aligned}
 & = \left[-\frac{t'^2}{8} I_0^c - \frac{t^c}{4} I_1^c + \frac{1}{2} I_2^c + \frac{1}{t^c} I_3^c \right] \dot{w}^t + \\
 & \left[\frac{t'^4}{16} I_0^c - \frac{t'^2}{2} I_2^c + I_4^c \right] \dot{w}_2^c + \left[\frac{t'^4}{16} I_1^c - \frac{t'^2}{2} I_3^c + I_5^c \right] \dot{w}_3^c \\
 & + \left[-\frac{t'^2}{8} I_0^c + \frac{t^c}{4} I_1^c + \frac{1}{2} I_2^c - \frac{1}{t^c} I_3^c \right] \dot{w}^b \\
 & - \left(\frac{h_x t'^{c2}}{4x} \right) \{M_x^c\} - \left(\frac{h_x t'^{c2}}{4} \right) \{M_{x,x}^c\} + \left(\frac{h_x}{x} \right) \{M_x^{*c}\} \\
 & + h_x \{M_{x,x}^{*c}\} + \left(\frac{h_\varphi t'^{c2}}{4x} \right) \{M_\varphi^c\} - \left(\frac{h_\varphi}{x} \right) \{M_\varphi^{*c}\} \\
 & - \left(\frac{h_x \varphi t'^{c2}}{4x \tan \alpha} \right) \{M_{\varphi x, \varphi}^c\} + \left(\frac{h_x \varphi}{x \sin \alpha} \right) \{M_{\varphi x, \varphi}^{*c}\} + \left(\frac{t'^2}{4} \right) \{Q_{zx}^c\}
 \end{aligned}$$

$$\begin{aligned}
 & - 3 \{Q_{zx}^{*c}\} = \left[-\frac{t'^2}{8} I_1^c - \frac{t^c}{4} I_2^c + \frac{1}{2} I_3^c + \frac{1}{t^c} I_4^c \right] \dot{u}_0^t \\
 & + \left[\frac{t'^2 t'}{16} I_1^c + \frac{t' t'^c}{8} I_2^c - \frac{t'}{4} I_3^c - \frac{t'}{2t^c} I_4^c \right] \ddot{\theta}_x^t \\
 & + \left[\frac{t'^4}{16} I_1^c - \frac{t'^2}{2} I_3^c + I_5^c \right] \dot{u}_2^c + \left[\frac{t'^4}{16} I_2^c - \frac{t'^2}{2} I_4^c + I_6^c \right] \dot{u}_3^c \\
 & + \left[-\frac{t'^2}{8} I_1^c + \frac{t^c}{4} I_2^c + \frac{1}{2} I_3^c - \frac{1}{t^c} I_4^c \right] \dot{u}_0^b + \\
 & \left[-\frac{t'^2 t^b}{16} I_1^c + \frac{t^c t^b}{8} I_2^c + \frac{t^b}{4} I_3^c - \frac{t^b}{2t^c} I_4^c \right] \ddot{\theta}_x^b
 \end{aligned} \tag{15i}$$

$$\begin{aligned}
 & \left(\frac{h_\varphi t'^{c2}}{4x \sin \alpha} \right) \{M_{\varphi, \varphi}^c\} + \left(\frac{h_\varphi}{x \sin \alpha} \right) \{M_{\varphi, \varphi}^{*c}\} - \left(\frac{h_x \varphi t'^{c2}}{4x} \right) \{M_{\varphi x}^c\} \\
 & - \left(\frac{h_x \varphi t'^{c2}}{4x} \right) \{M_{x\varphi}^c\} - \left(\frac{h_x \varphi t'^{c2}}{4} \right) \{M_{x\varphi, x}^c\} + \left(\frac{h_x \varphi}{x} \right) \{M_{\varphi x}^{*c}\} \\
 & + \left(\frac{h_x \varphi}{x} \right) \{M_{x\varphi}^{*c}\} + h_x \varphi \{M_{x\varphi, x}^{*c}\} - \left(\frac{t'^2}{4x \tan \alpha} \right) \{S_{\varphi z}^c\} \\
 & + \left(\frac{t'^2}{4} \right) \{Q_{z\varphi}^c\} + \left(\frac{1}{x \tan \alpha} \right) \{S_{\varphi z}^{*c}\} - 3 \{Q_{z\varphi}^{*c}\}
 \end{aligned}$$

$$\begin{aligned}
 & = \left[-\frac{t'^2}{8} I_1^c - \frac{t^c}{4} I_2^c + \frac{1}{2} I_3^c + \frac{1}{t^c} I_4^c \right] \dot{v}_0^t \\
 & + \left[\frac{t'^2 t'}{16} I_1^c + \frac{t' t'^c}{8} I_2^c - \frac{t'}{4} I_3^c - \frac{t'}{2t^c} I_4^c \right] \ddot{\theta}_\varphi^t + \\
 & \left[\frac{t'^4}{16} I_1^c - \frac{t'^2}{2} I_3^c + I_5^c \right] \dot{v}_2^c + \left[\frac{t'^4}{16} I_2^c - \frac{t'^2}{2} I_4^c + I_6^c \right] \dot{v}_3^c \\
 & + \left[-\frac{t'^2}{8} I_1^c + \frac{t^c}{4} I_2^c + \frac{1}{2} I_3^c - \frac{1}{t^c} I_4^c \right] \dot{v}_0^b +
 \end{aligned} \tag{15j}$$

$$\left[-\frac{t^{c^2}t^b}{16}I_1^c + \frac{t^c t^b}{8}I_2^c + \frac{t^b}{4}I_3^c - \frac{t^b}{2t^c}I_4^c \right] \ddot{\theta}_\varphi^b \quad (15j)$$

$$\begin{aligned} & \left(\frac{h_\varphi t^{c^2}}{4x \tan \alpha} \right) \{M_\varphi^c\} - \left(\frac{h_\varphi}{x \tan \alpha} \right) \{M_\varphi^{*c}\} + \left(\frac{t^{c^2}}{4} \right) \{N_z^c\} \\ & - 3\{N_z^{*c}\} - \left(\frac{t^{c^2}}{4x \sin \alpha} \right) \{S_{\varphi z}^c\} + \left(\frac{1}{x \sin \alpha} \right) \{S_{\varphi z, \varphi}^{*c}\} \\ & - \left(\frac{t^{c^2}}{4x} \right) \{S_{xz}^c\} - \left(\frac{t^{c^2}}{4} \right) \{S_{xz, x}^c\} + \left(\frac{1}{x} \right) \{S_{xz}^{*c}\} + \{S_{xz, x}^{*c}\} = \end{aligned} \quad (15k)$$

$$\begin{aligned} & \left[-\frac{t^{c^2}}{8}I_1^c - \frac{t^c}{4}I_2^c + \frac{1}{2}I_3^c + \frac{1}{t^c}I_4^c \right] \ddot{w}^t \\ & + \left[\frac{t^{c^4}}{16}I_1^c - \frac{t^{c^2}}{2}I_3^c + I_5^c \right] \ddot{w}_2^c + \left[\frac{t^{c^4}}{16}I_2^c - \frac{t^{c^2}}{2}I_4^c + I_6^c \right] \ddot{w}_3^c + \\ & \left[-\frac{t^{c^2}}{8}I_1^c + \frac{t^c}{4}I_2^c + \frac{1}{2}I_3^c - \frac{1}{t^c}I_4^c \right] \ddot{w}^b \end{aligned}$$

$$\begin{aligned} & \left(\frac{h_x}{2x} \right) \{N_x^c\} + \left(\frac{h_x}{2} \right) \{N_{x,x}^c\} - \left(\frac{h_x}{xt^c} \right) \{M_x^c\} - \left(\frac{h_x}{t^c} \right) \{M_{x,x}^c\} \\ & - \left(\frac{h_\varphi}{2x} \right) \{N_\varphi^c\} + \left(\frac{h_\varphi}{xt^c} \right) \{M_\varphi^c\} + \left(\frac{h_{x\varphi}}{2x \sin \varphi} \right) \{N_{\varphi x, \varphi}^c\} \\ & - \left(\frac{h_{x\varphi}}{x \sin \varphi^c} \right) \{M_{\varphi x, \varphi}^c\} + \left(\frac{1}{t^c} \right) \{Q_{zx}^c\} + \left(\frac{1}{x} \right) \{N_x^b\} + \{N_{x,x}^b\} \\ & - \left(\frac{1}{x} \right) \{N_\varphi^b\} + \left(\frac{1}{x \sin \varphi} \right) \{N_{\varphi x, \varphi}^b\} = \left[\frac{1}{4}I_0^c - \frac{1}{t^{c^2}}I_2^c \right] \ddot{u}_0^c \\ & + \left[-\frac{t^c}{8}I_0^c + \frac{t^c}{2t^{c^2}}I_2^c \right] \ddot{\theta}_x^c + \left[-\frac{t^{c^2}}{8}I_0^c + \frac{t^c}{4}I_1^c + \frac{1}{2}I_2^c - \frac{1}{t^c}I_3^c \right] \ddot{u}_2^c \\ & + \left[-\frac{t^{c^2}}{8}I_1^c + \frac{t^c}{4}I_2^c + \frac{1}{2}I_3^c - \frac{1}{t^c}I_4^c \right] \ddot{u}_3^c + \\ & \left[\left(\frac{1}{4}I_0^c - \frac{1}{t^c}I_1^c + \frac{1}{t^{c^2}}I_2^c \right) + I_0^b \right] \ddot{u}_0^b \\ & + \left[\left(\frac{t^b}{8}I_0^c - \frac{t^b}{2t^c}I_1^c + \frac{t^b}{2t^{c^2}}I_2^c \right) + I_1^b \right] \ddot{\theta}_x^b \end{aligned} \quad (15l)$$

$$\begin{aligned} & \left(\frac{h_\varphi}{2x \sin \alpha} \right) \{N_{\varphi, \varphi}^c\} - \left(\frac{h_\varphi}{t^c x \sin \alpha} \right) \{M_{\varphi, \varphi}^c\} + \left(\frac{h_{x\varphi}}{2x} \right) \{N_{x\varphi}^c\} \\ & + \left(\frac{h_{x\varphi}}{2} \right) \{N_{x\varphi, x}^c\} + \left(\frac{h_{x\varphi}}{2x} \right) \{N_{\varphi x}^c\} - \left(\frac{h_{x\varphi}}{xt^c} \right) \{M_{x\varphi}^c\} - \left(\frac{h_{x\varphi}}{t^c} \right) \{M_{x\varphi, x}^c\} \\ & - \left(\frac{h_{x\varphi}}{xt^c} \right) \{M_{\varphi x}^c\} + \left(\frac{1}{2x \tan \alpha} \right) \{Q_{\varphi z}^c\} - \left(\frac{1}{t^c x \tan \alpha} \right) \{S_{\varphi z}^c\} + \\ & \left(\frac{1}{t^c} \right) \{Q_{z\varphi}^c\} + \left(\frac{1}{x \sin \alpha} \right) \{N_{\varphi, \varphi}^b\} + \left(\frac{1}{x} \right) \{N_{x\varphi}^b\} + \{N_{x\varphi, x}^b\} \\ & + \left(\frac{1}{x} \right) \{N_{\varphi x}^b\} + \left(\frac{k_s}{x \tan \alpha} \right) \{Q_{\varphi z}^b\} = \left[\frac{1}{4}I_0^c - \frac{1}{t^{c^2}}I_2^c \right] \ddot{v}_0^c \\ & + \left[-\frac{t^c}{8}I_0^c + \frac{t^c}{2t^{c^2}}I_2^c \right] \ddot{\theta}_\varphi^c + \left[-\frac{t^{c^2}}{8}I_0^c + \frac{t^c}{4}I_1^c + \frac{1}{2}I_2^c - \frac{1}{t^c}I_3^c \right] \ddot{v}_2^c + \\ & \left[-\frac{t^{c^2}}{8}I_1^c + \frac{t^c}{4}I_2^c + \frac{1}{2}I_3^c - \frac{1}{t^c}I_4^c \right] \ddot{v}_3^c \\ & + \left[\left(\frac{1}{4}I_0^c - \frac{1}{t^c}I_1^c + \frac{1}{t^{c^2}}I_2^c \right) + I_0^b \right] \ddot{v}_0^b + \\ & \left[\left(\frac{t^b}{8}I_0^c - \frac{t^b}{2t^c}I_1^c + \frac{t^b}{2t^{c^2}}I_2^c \right) + I_1^b \right] \ddot{\theta}_\varphi^b \end{aligned} \quad (15m)$$

$$\begin{aligned} & - \left(\frac{h_\varphi}{2x \tan \alpha} \right) \{N_\varphi^c\} + \left(\frac{h_\varphi}{t^c x \tan \alpha} \right) \{M_\varphi^c\} + \left(\frac{1}{t^c} \right) \{N_z^c\} \\ & + \left(\frac{1}{2x} \right) \{Q_{xz}^c\} + \left(\frac{1}{2} \right) \{Q_{xz, x}^c\} - \left(\frac{1}{xt^c} \right) \{S_{xz}^c\} - \\ & \left(\frac{1}{t^c} \right) \{S_{xz, x}^c\} + \left(\frac{1}{2x \sin \alpha} \right) \{Q_{\varphi z, \varphi}^c\} - \left(\frac{1}{x \sin \alpha t^c} \right) \{S_{\varphi z, \varphi}^c\} \\ & - \left(\frac{1}{x \sin \alpha} \right) \{N_\varphi^b\} + \left(\frac{k_s}{x} \right) \{Q_{\varphi z}^b\} + k_s \{Q_{\varphi z, x}^b\} + \\ & \left(\frac{k_s}{x \tan \alpha} \right) \{Q_{\varphi z, \varphi}^b\} = \left[\frac{1}{4}I_0^c - \frac{1}{t^{c^2}}I_2^c \right] \ddot{w}^t \end{aligned} \quad (15n)$$

$$\begin{aligned} & + \left[-\frac{t^{c^2}}{8}I_0^c + \frac{t^c}{4}I_1^c + \frac{1}{2}I_2^c - \frac{1}{t^c}I_3^c \right] \ddot{w}_2^c + \\ & \left[-\frac{t^{c^2}}{8}I_1^c + \frac{t^c}{4}I_2^c + \frac{1}{2}I_3^c - \frac{1}{t^c}I_4^c \right] \ddot{w}_3^c \\ & + \left[\left(\frac{1}{4}I_0^c - \frac{1}{t^c}I_1^c + \frac{1}{t^{c^2}}I_2^c \right) + I_0^b \right] \ddot{w}^b \end{aligned}$$

$$\begin{aligned} & \left(\frac{h_x t^b}{4x} \right) \{N_x^c\} + \left(\frac{h_x t^b}{4} \right) \{N_{x,x}^c\} - \left(\frac{h_x t^b}{2xt^c} \right) \{M_x^c\} \\ & - \left(\frac{h_x t^b}{2t^c} \right) \{M_{x,x}^c\} - \left(\frac{h_\varphi t^b}{4x} \right) \{N_\varphi^c\} + \left(\frac{h_\varphi t^b}{2xt^c} \right) \{M_\varphi^c\} \\ & + \left(\frac{h_{x\varphi} t^b}{4x \sin \alpha} \right) \{N_{\varphi x, \varphi}^c\} - \left(\frac{h_{x\varphi} t^b}{2x \sin \alpha t^c} \right) \{M_{\varphi x, \varphi}^c\} + \left(\frac{t^b}{2t^c} \right) \{Q_{zx}^c\} \\ & + \left(\frac{1}{x} \right) \{M_x^b\} + \{M_{x,x}^b\} - \left(\frac{1}{x} \right) \{M_\varphi^b\} + \left(\frac{1}{x \sin \alpha} \right) \{M_{\varphi x, \varphi}^b\} \\ & - k_s \{Q_{zx}^b\} = \left[\frac{t^b}{8}I_0^c - \frac{t^b}{2t^{c^2}}I_2^c \right] \ddot{u}_0^b + \left[-\frac{t^b t^c}{16}I_0^c + \frac{t^b t^c}{4t^{c^2}}I_2^c \right] \ddot{\theta}_x^c + \end{aligned} \quad (15o)$$

$$\begin{aligned} & \left[-\frac{t^b t^{c^2}}{16}I_0^c + \frac{t^b t^c}{8}I_1^c + \frac{t^b}{4}I_2^c - \frac{t^b}{2t^c}I_3^c \right] \ddot{u}_2^c \\ & + \left[-\frac{t^b t^{c^2}}{16}I_1^c + \frac{t^b t^c}{8}I_2^c + \frac{t^b}{4}I_3^c - \frac{t^b}{2t^c}I_4^c \right] \ddot{u}_3^c + \\ & \left[\left(\frac{t^b}{8}I_0^c - \frac{t^b}{2t^c}I_1^c + \frac{t^b}{2t^{c^2}}I_2^c \right) + I_1^b \right] \ddot{u}_0^b \\ & + \left[\left(\frac{t^b t^c}{16}I_0^c - \frac{t^b t^c}{4t^c}I_1^c + \frac{t^b t^c}{4t^{c^2}}I_2^c \right) + I_2^b \right] \ddot{\theta}_x^b \end{aligned}$$

$$\begin{aligned} & \left(\frac{h_\varphi t^b}{4x \sin \alpha} \right) \{N_{\varphi, \varphi}^c\} - \left(\frac{h_\varphi t^b}{2x \sin \alpha t^c} \right) \{M_{\varphi, \varphi}^c\} + \left(\frac{h_{x\varphi} t^b}{4x} \right) \{N_{x\varphi}^c\} \\ & + \left(\frac{h_{x\varphi} t^b}{4x} \right) \{N_{x\varphi, x}^c\} + \left(\frac{h_{x\varphi} t^b}{4} \right) \{N_{\varphi x, \varphi}^c\} - \left(\frac{h_{x\varphi} t^b}{2xt^c} \right) \{M_{\varphi x}^c\} \\ & - \left(\frac{h_{x\varphi} t^b}{2xt^c} \right) \{M_{x\varphi, \varphi}^c\} - \left(\frac{h_{x\varphi} t^b}{2t^c} \right) \{M_{x\varphi, x}^c\} + \left(\frac{t^b}{4x \tan \alpha} \right) \{Q_{\varphi z}^c\} \\ & - \left(\frac{t^b}{2t^c x \tan \alpha} \right) \{S_{\varphi z}^c\} + \left(\frac{t^b}{2t^c} \right) \{Q_{z\varphi}^c\} + \left(\frac{1}{x \sin \alpha} \right) \{M_{\varphi, \varphi}^b\} \\ & + \left(\frac{1}{x} \right) \{M_{\varphi x}^b\} + \left(\frac{1}{x} \right) \{M_{x\varphi}^b\} + \{M_{x\varphi, x}^b\} + \left(\frac{k_s}{x \tan \alpha} \right) \{S_{\varphi z}^b\} \\ & - k_s \{Q_{z\varphi}^b\} = \left[\frac{t^b}{8}I_0^c - \frac{t^b}{2t^{c^2}}I_2^c \right] \ddot{v}_0^c + \left[-\frac{t^b t^c}{16}I_0^c + \frac{t^b t^c}{4t^{c^2}}I_2^c \right] \ddot{\theta}_\varphi^c \\ & + \left[-\frac{t^b t^{c^2}}{16}I_0^c + \frac{t^b t^c}{8}I_1^c + \frac{t^b}{4}I_2^c - \frac{t^b}{2t^c}I_3^c \right] \ddot{v}_2^c + \end{aligned} \quad (15p)$$

$$\begin{aligned} & \left[-\frac{t^b t^c}{16} I_1^c + \frac{t^b t^c}{8} I_2^c + \frac{t^b}{4} I_3^c - \frac{t^b}{2t^c} I_4^c \right] \ddot{v}_3^c \\ & + \left[\left(\frac{t^b}{8} I_0^c - \frac{t^b}{2t^c} I_1^c + \frac{t^b}{2t^c} I_2^c \right) + I_1^b \right] \ddot{v}_0^b \\ & + \left[\left(\frac{t^{b2}}{16} I_0^c - \frac{t^{b2}}{4t^c} I_1^c + \frac{t^{b2} I_2^c}{4t^c} \right) + I_2^b \right] \ddot{\theta}_\varphi^b \end{aligned} \quad (15p)$$

In above relations, the components of the resultant forces and moments per unit of the length which act along the lines of the constant x or φ in the face sheets and the core of STCS can be defined as

$$\begin{aligned} & \begin{bmatrix} N_x^c & N_x^{*c} & M_x^c & M_x^{*c} \\ N_\varphi^c & N_\varphi^{*c} & M_\varphi^c & M_\varphi^{*c} \\ N_z^c & N_z^{*c} & M_z^c & 0 \\ N_{x\varphi}^c & N_{x\varphi}^{*c} & M_{x\varphi}^c & M_{x\varphi}^{*c} \\ N_{\varphi x}^c & N_{\varphi x}^{*c} & M_{\varphi x}^c & M_{\varphi x}^{*c} \end{bmatrix} \\ & = \int_z \begin{bmatrix} k_2^c & 0 & 0 & 0 \\ 0 & k_1^c & 0 & 0 \\ 0 & 0 & k_1^c k_2^c & 0 \\ 0 & 0 & 0 & k_2^c \\ 0 & 0 & 0 & 0 \end{bmatrix} \begin{bmatrix} \sigma_x \\ \sigma_\varphi \\ \sigma_z \\ \tau_{x\varphi} \\ \tau_{\varphi x} \end{bmatrix}^c (1, z^2, z, z^3) dz \end{aligned} \quad (16)$$

$$\begin{aligned} & \begin{bmatrix} Q_{\varphi z}^c & Q_{\varphi z}^{*c} & S_{\varphi z}^c & S_{\varphi z}^{*c} \\ Q_{z\varphi}^c & Q_{z\varphi}^{*c} & S_{z\varphi}^c & 0 \\ Q_{xz}^c & Q_{xz}^{*c} & S_{xz}^c & S_{xz}^{*c} \\ Q_{zx}^c & Q_{zx}^{*c} & S_{zx}^c & 0 \end{bmatrix} \\ & = \int_z \begin{bmatrix} k_1^c & 0 & 0 & 0 \\ 0 & k_1^c k_2^c & 0 & 0 \\ 0 & 0 & k_2^c & 0 \\ 0 & 0 & 0 & k_1^c k_2^c \end{bmatrix} \begin{bmatrix} \tau_{\varphi z} \\ \tau_{z\varphi} \\ \tau_{xz} \\ \tau_{zx} \end{bmatrix}^c (1, z^2, z, z^3) dz \end{aligned} \quad (17)$$

$$\begin{aligned} & \begin{bmatrix} N_x^i & M_x^i \\ N_\varphi^i & M_\varphi^i \\ N_{x\varphi}^i & M_{x\varphi}^i \\ N_{\varphi x}^i & M_{\varphi x}^i \end{bmatrix} = \int_{z^i} \begin{bmatrix} k_2^i & 0 & 0 & 0 \\ 0 & k_1^i & 0 & 0 \\ 0 & 0 & k_2^i & 0 \\ 0 & 0 & 0 & k_1^i \end{bmatrix} \begin{bmatrix} \sigma_x \\ \sigma_\varphi \\ \tau_{x\varphi} \\ \tau_{\varphi x} \end{bmatrix}^i (1, z^i) dz^i \end{aligned} \quad (18)$$

$$\begin{aligned} & \begin{bmatrix} Q_{\varphi z}^i & S_{\varphi z}^i \\ Q_{z\varphi}^i & 0 \\ Q_{xz}^i & S_{xz}^i \\ Q_{zx}^i & 0 \end{bmatrix} = \int_{z^i} \begin{bmatrix} k_1^i & 0 & 0 & 0 \\ 0 & k_1^i k_2^i & 0 & 0 \\ 0 & 0 & k_2^i & 0 \\ 0 & 0 & 0 & k_1^i k_2^i \end{bmatrix} \begin{bmatrix} \tau_{\varphi z} \\ \tau_{z\varphi} \\ \tau_{xz} \\ \tau_{zx} \end{bmatrix}^i (1, z^i) dz^i \end{aligned} \quad (19)$$

where

$$k_1^c = 1, \quad k_2^c = \left(1 + C_1 \frac{z^c}{R_\varphi} \right) \quad (20)$$

$$k_1^i = 1, \quad k_2^i = \left(1 + C_1 \frac{z^i}{R_\varphi} \right), \quad i = t, b \quad (21)$$

Substituting Eqs. (19)-(21) into Eqs. (1) and (4) and combining with Eqs. (16)-(19) yields

$$\{\bar{F}\} = [D]\{\bar{\Xi}\} \quad (22)$$

in which

$$\begin{aligned} [D] &= \begin{bmatrix} [D_f^i]_{a \times a} & 0 \\ 0 & k_o [D_s^i]_{b \times b} \end{bmatrix}, \\ [D_f^i] &= \begin{bmatrix} [A]_{c \times c}^i & [B]_{c \times d}^i \\ [E]_{d \times c}^i & [D]_{d \times d}^i \end{bmatrix} \end{aligned} \quad (23)$$

Dimensions of the matrix D for the core are: $a = 19$, $b = 14$, $c = 10$, $d = 9$, and for the face sheets are: $a = 8$, $b = 8$, $c = 4$, $d = 4$. Also, the elements of $[D]$ for the core and the face sheets are given in Appendix A. In addition, k_o parameter is called as shear correction factor of FSDT which is equal to 5/6 (Reissner 1953). Components of \bar{F} and $\bar{\Xi}$ for the face sheets and the core are defined as

$$\{\bar{\epsilon}_c\} = \begin{bmatrix} \epsilon_{0\alpha}^c, \epsilon_{0\beta}^c, \epsilon_{0\beta\alpha}^c, \epsilon_{0\alpha\beta}^c, \epsilon_{0\alpha}^{*c}, \epsilon_{0\beta}^{*c}, \epsilon_{0\beta\alpha}^{*c}, \epsilon_{0\alpha\beta}^{*c}, \\ \epsilon_{0z}^c, \epsilon_{0z}^{*c}, \kappa_\alpha^c, \kappa_\beta^c, \chi_{\beta\alpha}^c, \chi_{\alpha\beta}^c, \kappa_\alpha^{*c}, \kappa_\beta^{*c}, \chi_{\beta\alpha}^{*c}, \chi_{\alpha\beta}^{*c}, \\ \kappa_z^c, \epsilon_{0z\alpha}^c, \epsilon_{0\alpha z}^c, \epsilon_{0z\beta}^c, \epsilon_{0\beta z}^c, \epsilon_{0z\alpha}^{*c}, \epsilon_{0z\beta}^{*c}, \\ \epsilon_{0\alpha z}^{*c}, \epsilon_{0\beta z}^{*c}, \chi_{z\alpha}^c, \chi_{\alpha z}^c, \chi_{z\beta}^c, \chi_{\beta z}^c, \chi_{\alpha z}^{*c}, \chi_{\beta z}^{*c} \end{bmatrix}^T \quad (24)$$

$$\{\bar{\sigma}_c\} = \begin{bmatrix} N_\alpha^c, N_\beta^c, N_{\beta\alpha}^c, N_{\alpha\beta}^c, N_\alpha^{*c}, N_\beta^{*c}, N_{\beta\alpha}^{*c}, N_{\alpha\beta}^{*c}, \\ N_z^c, N_z^{*c}, M_\alpha^c, M_\beta^c, M_{\beta\alpha}^c, M_{\alpha\beta}^c, M_\alpha^{*c}, M_\beta^{*c}, \\ M_{\beta\alpha}^{*c}, M_{\alpha\beta}^{*c}, M_z^c, Q_{z\alpha}^c, Q_{\alpha z}^c, Q_{z\beta}^c, Q_{\beta z}^c, Q_{z\alpha}^{*c}, Q_{z\beta}^{*c}, \\ Q_{\alpha z}^{*c}, Q_{\beta z}^{*c}, S_{z\alpha}^c, S_{\alpha z}^c, S_{z\beta}^c, S_{\beta z}^c, S_{\alpha z}^{*c}, S_{\beta z}^{*c} \end{bmatrix}^T \quad (25)$$

$$\{\bar{\epsilon}_i\} = \begin{bmatrix} \epsilon_{0\alpha}^i, \epsilon_{0\beta}^i, \epsilon_{0\beta\alpha}^i, \epsilon_{0\alpha\beta}^i \\ \kappa_\alpha^i, \kappa_\beta^i, \chi_{\beta\alpha}^i, \chi_{\alpha\beta}^i \\ \epsilon_{0z\alpha}^i, \epsilon_{0\alpha z}^i, \epsilon_{0z\beta}^i \\ \epsilon_{0\beta z}^i, \chi_{\alpha z}^i, \chi_{z\beta}^i \end{bmatrix}^T, \quad \text{that } i = t, b \quad (26)$$

$$\{\bar{\sigma}_i\} = \begin{bmatrix} N_\alpha^i, N_\beta^i, N_{\beta\alpha}^i, N_{\alpha\beta}^i \\ M_\alpha^i, M_\beta^i, M_{\beta\alpha}^i, M_{\alpha\beta}^i \\ Q_{z\alpha}^i, Q_{\alpha z}^i, Q_{z\beta}^i, Q_{\beta z}^i \\ S_{\alpha z}^i, S_{z\beta}^i \end{bmatrix}^T, \quad \text{that } i = t, b \quad (27)$$

Superscript T denotes the transpose. The considered boundary conditions (BCs) in this study are

➤ **Simply-simply BC**

$$\begin{aligned} v^i &= w^i = v_2^c = v_3^c = w_2^c = w_3^c \\ &= N_x^j = M_x^j = N_x^{*c} = M_x^{*c} = 0, \end{aligned} \quad (28)$$

on both ends $j = t, b, c$ and $i = t, b$

➤ **Clamped-Clamped BC**

$$\begin{aligned} u^i &= v^i = w^i = u_2^c = u_3^c = v_2^c = v_3^c = w_2^c = w_3^c \\ &= \frac{\partial w^i}{\partial x} = \frac{\partial w_2^c}{\partial x} = \frac{\partial w_3^c}{\partial x} = 0, \end{aligned} \quad (29)$$

on both ends $j = t, b, c$ and $i = t, b$

➤ **Clamped-Simply BC**

$$\begin{aligned} u^i &= v^i = w^i = u_2^c = u_3^c = v_2^c = v_3^c = w_2^c = w_3^c \\ &= \frac{\partial w^i}{\partial x} = \frac{\partial w_2^c}{\partial x} = \frac{\partial w_3^c}{\partial x} = 0, \quad \text{at } x = 0 \end{aligned} \quad (30)$$

$$v^i = w^i = v_2^c = v_3^c = w_2^c = w_3^c = 0, \quad \text{at } x = L \quad (30)$$

$$j = t, b, c \quad \text{and} \quad i = t, b$$

where $j = t, b, c$ and $i = t, b$.

4. Low-velocity impact response

As shown in Fig. 2, the three-degrees-of-freedom (TDOF) spring–mass–damper (SMD) model is applied to predict the low-velocity impact response of STCS.

The motion equations of the three-TDOF system can be written as follows

$$M_I \ddot{\Delta}_0 + K_C^* (\Delta_0 - \Delta_1) = 0, \quad (31)$$

$$\begin{aligned} \bar{M}_{face} \ddot{\Delta}_1 + K_{face} \Delta_1 + K_{face} (\Delta_1 - \Delta_2) \\ + K_C^* (\Delta_1 - \Delta_0) = 0, \end{aligned} \quad (32)$$

$$\begin{aligned} \bar{M}_{sand} \ddot{\Delta}_2 + K_{sand} \Delta_2 + C_{ef} \dot{\Delta}_2 \\ + K_{core} (\Delta_2 - \Delta_1) = 0, \end{aligned} \quad (33)$$

where Δ_0, Δ_1 and Δ_2 are transverse displacements of the impactor, impacted top and bottom face sheets, respectively; M_I, \bar{M}_{face} and \bar{M}_{sand} are the mass of the impactor, the effective mass of impacted face sheet and the effective mass of STCS, respectively; $K_C^*, K_{face}, K_{sand}$ and K_{core} are respectively, the effective stiffness of the contact, the face sheet, STCS and the core, C_{ef} is the effective viscous damping coefficient which can be defined as Malekzadeh *et al.* (2006)

$$C_{ef} = \eta_{st} (K_{sand} / \omega_1), \quad (34)$$

where η_{st} and ω_1 are damping coefficient and fundamental natural frequency of structure, respectively.

The effective stiffness of the impactor can be expressed as

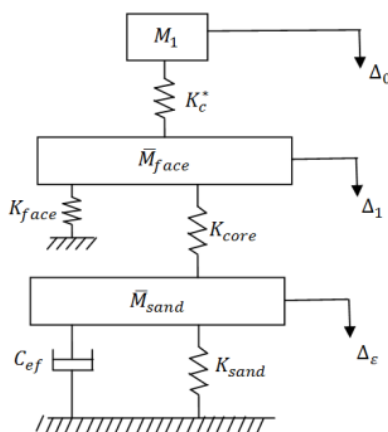


Fig. 2 The equivalent TDOF model of the structure and the impactor system (SMD model)

$$K_C^* = \sqrt{\pi} \Gamma \left(\frac{P+1}{P} \right) \frac{2\Gamma \left(\frac{P+1}{2} \right) + \sqrt{\pi} \Gamma \left(\frac{P+1}{2} \right)}{4\Gamma^2 \left(\frac{P+1}{2} \right) + \sqrt{\pi} \Gamma^2 \left(\frac{P+1}{2} \right)} \alpha_{max}^{P-1} K_C, \quad (35)$$

where Γ is gamma function; P is Hertzian indentation (usually $P = 1.5$), α_{max} is a parameter which can be written as

$$\alpha_{max} = \left(\frac{\bar{M}_{sand} \cdot M_1}{\bar{M}_{sand} + M_1} \right)^{\frac{1}{(P+1)}} \left(\frac{P+1}{2} \right)^{\frac{1}{(P+1)}} \left(\frac{V_0^2}{K_C} \right)^{\frac{1}{(P+1)}} \quad (36)$$

where V_0 is the impact velocity of impactor and the contact stiffness (K_C) may be estimated as

$$K_C = \left(\frac{4}{3} \right) ER_I^{1/2}, \quad \frac{1}{E} = \frac{1 - \nu_I^2}{E_I} + \frac{1 - \nu_P^2}{E_P} \quad (37)$$

where R_I, E_I and ν_I are the radius, the elastic modulus and poisson's ratio of the impactor, respectively; E_P and ν_P are elastic modulus and poisson's ratio of structure, respectively.

The effective compressive stiffness of the elastic flexible core can be given as follows (Malekzadeh *et al.* 2007)

$$K_{core} = 8 \sqrt{k_F D_f^*} \quad (38)$$

where k_F is the foundation stiffness (elastic region of the core is modeled as a Winkler foundation) and D_f^* is the effective stiffness of the impacted face sheet which can be written as

$$D_f^* = \sqrt{D_{11} D_{22} (\gamma + 1) / 2} \quad (39)$$

$$\gamma = (D_{12} + 2D_{66}) / \sqrt{D_{11} D_{22}} \quad (40)$$

$$k_F = \frac{E_c}{\bar{h}_c} \quad (41)$$

where \bar{h}_c can be expressed as

$$\bar{h}_c = \frac{h_c}{1.38} \quad \text{for } h_c \leq h_{c \max} \quad (42)$$

$$\text{and } \bar{h}_c = 2h_{c \max} \quad \text{for } h_c > h_{c \max}$$

$$\bar{h}_c = \left(\frac{27}{64} \right)^2 2h_{c \max} \quad \text{for } h_c > h_{c \max} \quad (43)$$

$$h_{c \max} \approx h_f \left(\frac{32}{27} \right) \left(\frac{4Q_f^*}{3E_c} \right)^{1/3} \quad \text{where } Q_f^* = \frac{12D_f^*}{h_f^3} \quad (44)$$

where h_f is the thickness of the impacted face sheet. The system of ordinary differential Eq. (6) can be solved analytically using the following initial conditions

$$\Delta_0(t = 0) = 0, \quad \Delta_1(t = 0) = 0, \quad \Delta_2(t = 0) = 0, \quad (45)$$

$$\dot{\Delta}_0(t = 0) = V_0, \quad \dot{\Delta}_1(t = 0) = 0, \quad \dot{\Delta}_2(t = 0) = 0, \quad (46)$$

Table 1 Material property of face sheets and core

Material properties	Face sheets	core
	$E_1 = 131 \text{ GPa}, E_2 = E_3 = 10.34 \text{ GPa}$	$E_1 = E_2 = E_3 = 0.00689 \text{ GPa}$
(0/90/core/0/90)	$G_{12} = G_{13} = 6.895 \text{ GPa}, G_{13} = 6.205 \text{ GPa}$	$G_{12} = G_{13} = G_{23} = 3.45 \text{ GPa}$
	$\nu_{12} = \nu_{13} = 0.22, \nu_{23} = 0.49, \rho = 1627 \text{ kg / m}^3$	$\nu = 0, \rho = 94.195 \text{ kg / m}^3$

By applying the equivalent damping concept due to Gong and Lam (2000), the eigenvalue equation can be obtained. Therefore

$$\begin{aligned}
 & (M_I \bar{M}_{face} \bar{M}_{sand}) \lambda^3 \\
 & - [K_{gbc} \bar{M}_{face} M_I + K_{gcc} \bar{M}_{sand} M_I + K_C^* \bar{M}_{face} \bar{M}_{sand}] \lambda^2 \\
 & + \left[\begin{aligned} & M_I (K_{gcc} K_{gbc} - K_{core}^2) \\ & + K_C^* (K_{gbc} \bar{M}_{face} + K_{gcc} \bar{M}_{sand}) - K_C^{*2} \bar{M}_{sand} \end{aligned} \right] \lambda^* \\
 & + [K_C^{*2} K_{gbc} - K_C^* (K_{gcc} K_{gbc} - K_{core}^2)] = 0
 \end{aligned} \tag{47}$$

where

$$K_{gcc} = K_{face} + K_{core} + K_C^* \tag{48}$$

$$K_{gbc} = K_{sand} (1 + \eta_{stj}) + K_{core} \tag{49}$$

$$j = \sqrt{-1} \tag{50}$$

The above eigenvalue equation has complex coefficients of $\lambda^* = \lambda' + i\lambda''$, where the circular frequency is $\omega = \sqrt{\lambda'}$. Finally, the equivalent contact force can be obtained as

$$F_C^*(t) = K_C^* \begin{bmatrix} c_1(\phi_0^1 - 1) \sin(\omega_1 t) \\ + c_2(\phi_0^2 - 1) \sin(\omega_2 t) \\ + c_3(\phi_0^3 - 1) \sin(\omega_3 t) \end{bmatrix} \tag{51}$$

where

$$\begin{aligned}
 \phi_0^i &= \text{real} \left(\frac{K_C^*}{K_C^* - M_I \lambda^*} \right), \\
 \phi_2^i &= \text{real} \left(\frac{K_{core}}{K_{gbc} - \bar{M}_{sand}^* \lambda^*} \right), \quad i = 1, 2, 3
 \end{aligned} \tag{52}$$

$$\begin{aligned}
 c_1 &= \frac{-V_0(\phi_2^2 - \phi_2^3)}{\omega_1[(\phi_0^2 - \phi_0^1)(\phi_2^1 - \phi_2^3) - (\phi_2^2 - \phi_2^1)(\phi_0^1 - \phi_0^3)]} \\
 &= \frac{-V_0(\phi_2^2 - \phi_2^3)}{\omega_1[(\phi_0^2 - \phi_0^1)(\phi_2^1 - \phi_2^3) - (\phi_2^2 - \phi_2^1)(\phi_0^1 - \phi_0^3)]}
 \end{aligned} \tag{53}$$

$$\begin{aligned}
 c_2 &= \frac{V_0(\phi_2^1 - \phi_2^3)}{\omega_2[(\phi_0^2 - \phi_0^1)(\phi_2^1 - \phi_2^3) - (\phi_2^2 - \phi_2^1)(\phi_0^1 - \phi_0^3)]} \\
 &= \frac{V_0(\phi_2^1 - \phi_2^3)}{\omega_2[(\phi_0^2 - \phi_0^1)(\phi_2^1 - \phi_2^3) - (\phi_2^2 - \phi_2^1)(\phi_0^1 - \phi_0^3)]}
 \end{aligned} \tag{54}$$

$$\begin{aligned}
 c_3 &= \frac{-V_0(\phi_2^1 - \phi_2^2)}{\omega_2[(\phi_0^2 - \phi_0^1)(\phi_2^1 - \phi_2^3) - (\phi_2^2 - \phi_2^1)(\phi_0^1 - \phi_0^3)]} \\
 &= \frac{-V_0(\phi_2^1 - \phi_2^2)}{\omega_2[(\phi_0^2 - \phi_0^1)(\phi_2^1 - \phi_2^3) - (\phi_2^2 - \phi_2^1)(\phi_0^1 - \phi_0^3)]}
 \end{aligned} \tag{55}$$

5. DQM

The DQM approximates the partial derivative of a function F , with respect to two spatial variables (x and φ) at a given discrete point (x_i, φ_i), as a weighted linear sum of

the function values at all discrete points chosen in the solution domain ($0 < x < L, 0 < \varphi < 2\pi$) with $N_x \times N_\varphi$ grid points along x and φ axes, respectively. Then, the n^{th} -order partial derivative of $F(x, \varphi)$ with respect to x , the m^{th} -order partial derivative of $F(x, \varphi)$ with respect to φ and the $(n + m)^{\text{th}}$ -order partial derivative of $F(x, \varphi)$ with respect to both x and φ is expressed discretely at the point (x_i, φ_i) as (Kolahchi *et al.* 2016, Kolahchi and Bidgoli 2016, Ghorbanpour Arani *et al.* 2015)

$$\frac{d^n F(x_i, \varphi_j)}{dx^n} = \sum_{k=1}^{N_x} A_{ik}^{(n)} F(x_k, \varphi_j) \quad n = 1, \dots, N_x - 1, \tag{56}$$

$$\frac{d^m F(x_i, \varphi_j)}{d\varphi^m} = \sum_{l=1}^{N_\varphi} B_{jl}^{(m)} F(x_i, \varphi_l) \quad m = 1, \dots, N_\varphi - 1, \tag{57}$$

$$\frac{d^{n+m} F(x_i, \varphi_j)}{dx^n d\varphi^m} = \sum_{k=1}^{N_x} \sum_{l=1}^{N_\varphi} A_{ik}^{(n)} B_{jl}^{(m)} F(x_k, \varphi_l), \tag{58}$$

where $A_{ik}^{(n)}$ and $B_{jl}^{(m)}$ are the weighting coefficients (Kolahchi *et al.* 2016).

Considering structural damping ($C_{ij} \rightarrow C_{ij} (1 + g \partial / \partial t)$ where g is structural damping), using Eqs. (53)-(63), the motion equations for low velocity impact of STCS can be expressed in matrix form as

$$[M]\{\ddot{\chi}\} + [C_e]\{\dot{\chi}\} + [K]\{\chi\} = \{Q\} \tag{58}$$

where $[M]$, $[K]$ and $[C_e]$ are the mass, stiffness and damp matrixes, respectively; Q is the dynamic load vector, and $\chi = \{u_0^t, v_0^t, w^t, \theta_x^t, \theta_\varphi^t, u_2^c, v_2^c, w_2^c, u_3^c, v_3^c, w_3^c, u_0^b, v_0^b, w^b, \theta_x^b, \theta_\varphi^b\}$ is the displacement vector. Defining the second and first time derivatives using Teoplitz matrices, Eq. (64) can be written as

$$([D_t^2 \otimes M] + [D_t^1 \otimes C_e] + [I_t \otimes K])\chi = [Q], \tag{60}$$

where \otimes notes the Kronecker product and I_t is unit matrix. Finally, solving above equation yields the deflection and the contact force of the structure which are discussed in the next section.

6. Numerical results and discussion

Based on the numerical solution outlined in section 5, the contact force and the deflection of the STCS are obtained. For this purpose, a sandwich laminated cone with $[0, 90]$ face sheet, length to outer radius $L/r_2 = 0.5$,

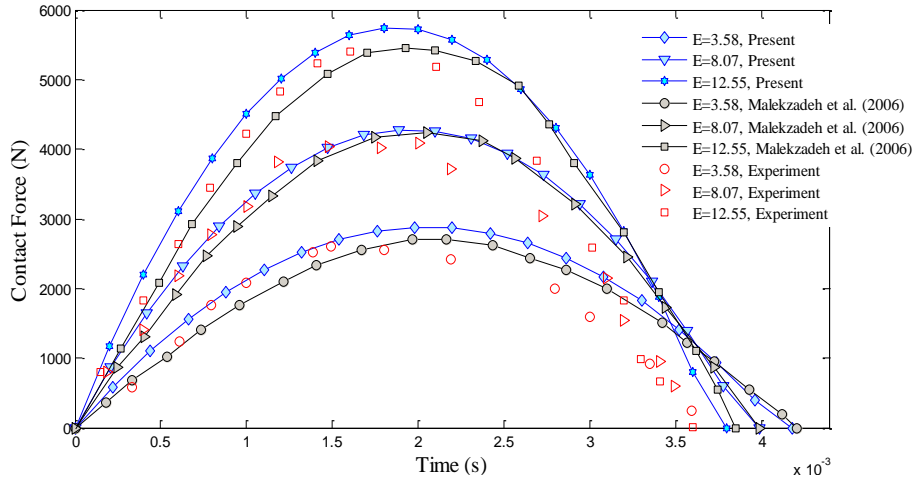


Fig. 3 Comparison of contact force history between present work and Anderson (2005) and Malekzadeh *et al.* (2006)

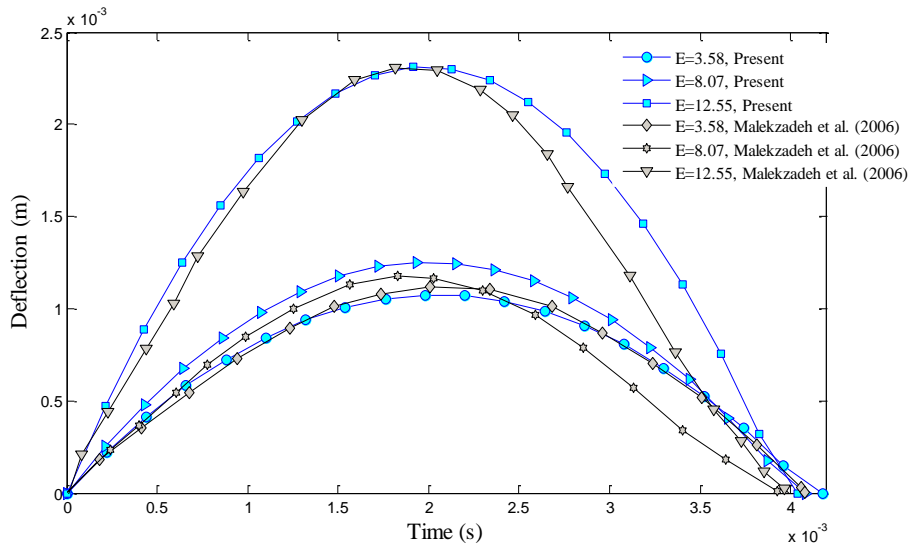


Fig. 4 Comparison of deflection history between present work and Anderson (2005) and Malekzadeh *et al.* (2006)

thickness to outer radius $h/r_2 = 0.1$ and cone semi vertex angle of 45° under the low velocity impact with velocity of $V = 1$ m/s, mass of impactor $M_I = 6.15$ Kg and damping coefficient $\eta_{st} = 0.47$ is considered. The orthotropic material properties of the face sheets and the core are chosen as shown in Table 1 (Tong 1994).

6.1 Validation

Before analysis the effects of different parameters on the dynamic response of the structure, the accuracy of present model should be investigated. To verify the present analysis, the results obtained for the case of a panel subjected to low velocity impact are compared with those reported experimentally by Anderson (2005) and numerically by Malekzadeh *et al.* (2006). Consider a $[0_2/90_2/0_2/core/0_2/90_2/0_2]$ panel with the core thickness of 12.7 mm, the overall dimensions of 76.2×76.2 mm, the thickness of the face sheets is 0.264 mm, the impactor mass is 1.8 kg, the impactor diameter is 25.4 mm and different the initial potential energy levels of the impactors are 3.58, 8.07, and

12.55 J. Figs. 3 and 4 illustrate respectively, the comparison of the contact force and the deflection histories of the structure for different initial potential energy levels of the impactor obtained in the present work with those reported

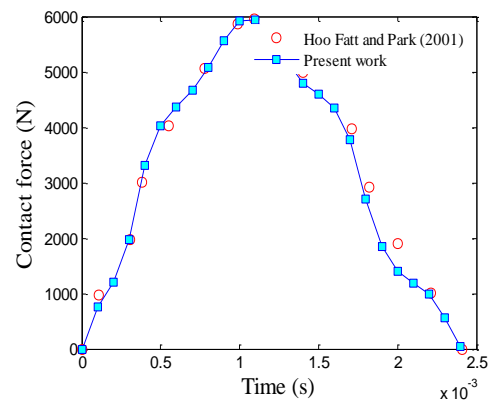


Fig. 5 Comparison of deflection history between present work and Fatt and Park (2001)

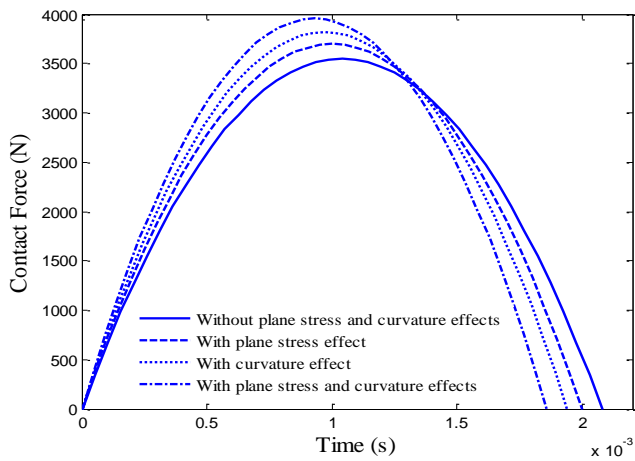


Fig. 6 The effect of curvature and in-plane stresses of core on the history of contact force

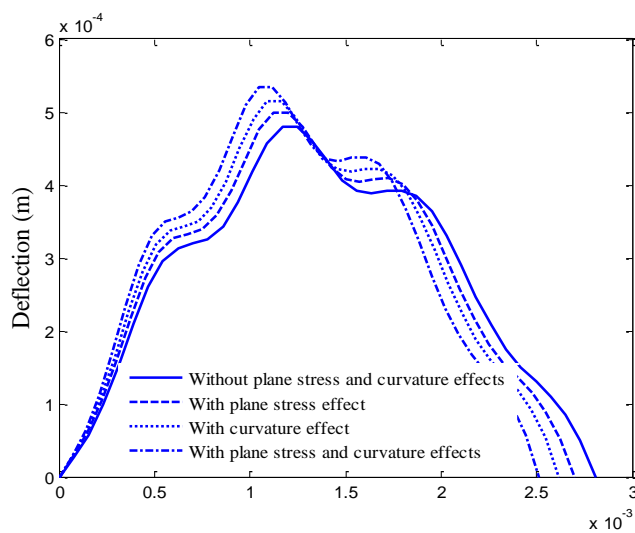


Fig. 7 The effect of curvature and in-plane stresses of core on the history of deflection

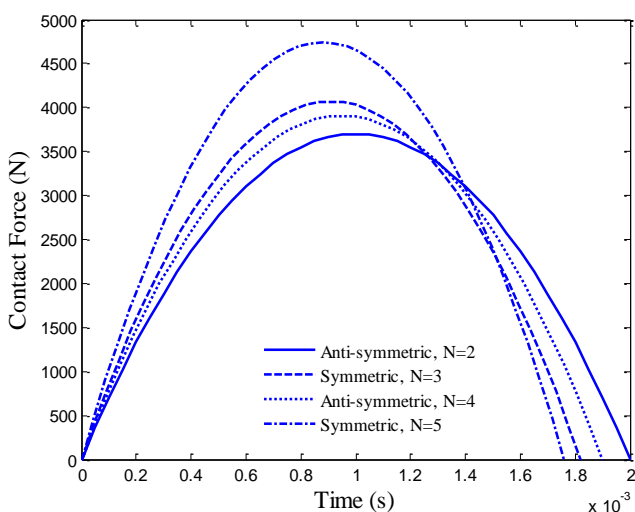


Fig. 8 The effect of layer number of face sheets on the history of contact force

by Anderson (2005) and Malekzadeh *et al.* (2006), experimentally and numerically, respectively. There are only small discrepancies between the predicted present analysis and those obtained by Anderson (2005) and Malekzadeh *et al.* (2006), indicating validation of this work.

In the next example, the proposed high-order model of this work is compared with the experimental results of Fatt and Park (2001). Considering thickness of core 12.7 mm and overall dimensions of 76.2×76.2 mm and the material properties the same as Ref. (2001), the contact force obtained by the DQM in this study is compared with the experimental contact force of Fatt and Park (2001) in Fig. 5. There are only small differences in the phase and the magnitude of the contact force obtained from the present analysis and the experimental results of Fatt and Park (2001), indicating validation of this work.

6.2 Curvature and core in-plane stresses effects

Figs. 6 and 7 shows, respectively the contact force and the central deflection histories of the structure for four cases including without considering the curvature and the in-plane stresses of the core effects, with considering the in-plane stresses of the core and neglecting the curvature effects, with considering the curvature effects and neglecting the in-plane stresses of the core effects. As can be seen from these figures, considering the curvature and the in-plane stresses of the core effects increases the contact force and the deflection of the sandwich structure while the contact duration decreases. The reason is that considering the curvature and the in-plane stresses of the core makes the structure stiffer which requires a larger deflection and accompanying the contact force to dissipate it. It is also concluded that the contact force and deflection of the case by considering the curvature effects and neglecting the in-plane stresses of the core are higher than the case of considering in-plane stresses of the core and neglecting the curvature effects due to low shell curvature.

6.3 Layer number of the face sheets effects

Figs. 8 and 9 present the histories of contact force and deflection of STCS for different layer number of the face sheets, respectively. The odd and even numbers indicate the symmetric and anti-symmetric laminate, respectively.

Because the stability of symmetric laminatet is more than that of the anti-symmetric one, the maximum contact force and deflection of symmetric lamina are slightly greater than that of the anti-symmetric one, while the contact duration for symmetric laminatet is slightly less than that for the anti-symmetric one. Interestingly, the maximum contact force and deflection of 3-layers laminate are higher than that of the 4-layers one which shows the importance of the structural balance.

6.4 Orientation angle of the face sheets effects

The effect of orientation angle of the face sheets on the contact force and deflection histories of the structure is

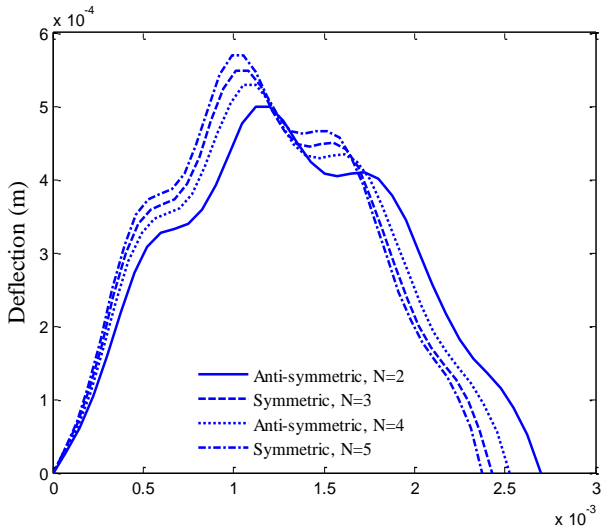


Fig. 9 The effect of face sheets layer number on the history of deflection

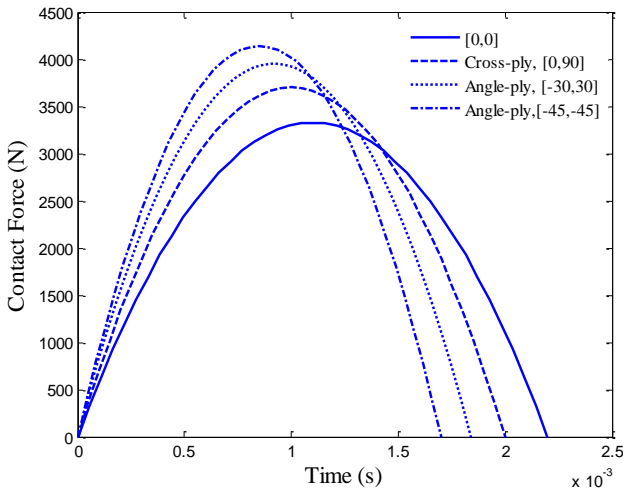


Fig. 10 The effect of face sheets orientation angle on the history of contact force

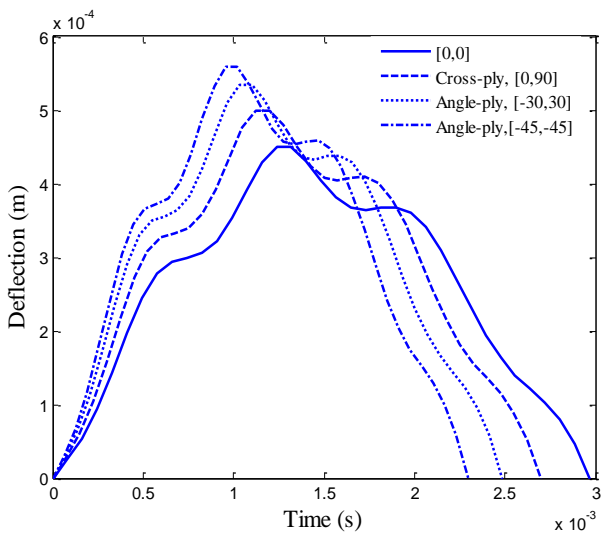


Fig. 11 The effect of face sheets orientation angle on the history of deflection

shown Figs. 10 and 11, respectively. Four cases of two-layers laminated conical shell are assumed as $(0^\circ, 0^\circ)$, cross ply type of $(0^\circ, 90^\circ)$, angle-ply types of $(30^\circ, -30^\circ)$ and $(45^\circ, -45^\circ)$. It is evident that the maximum contact force and deflection of angle-ply are higher than cross-ply type. As results, the angle-ply type laminated structure leads to higher stiffness and consequently higher maximum contact force and deflection. In addition, the angle-ply laminate shortens slightly the contact duration.

6.5 Cone semi vertex angle effects

The effect of the cone semi vertex angle on the contact force and deflection histories is demonstrated in Figs. 12 and 13, respectively. The figure shows that the contact force and the central deflection of the structure increases and the contact time decreases with increasing cone semi vertex angle. This behavior is due to the increase of the stiffness of the STCS with increasing cone semi vertex angle.

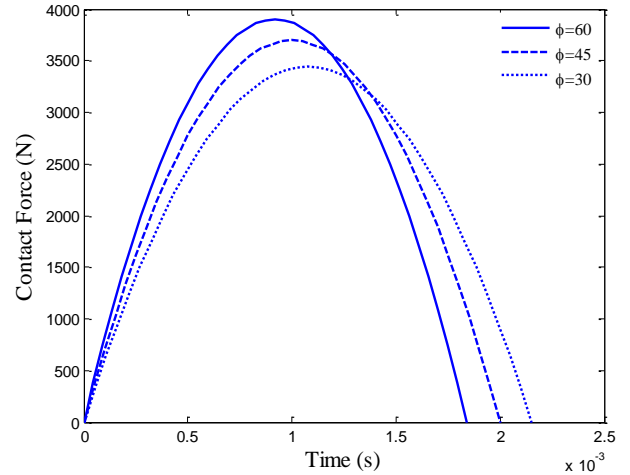


Fig. 12 The effect of core semi-vertex angle on the history of contact force

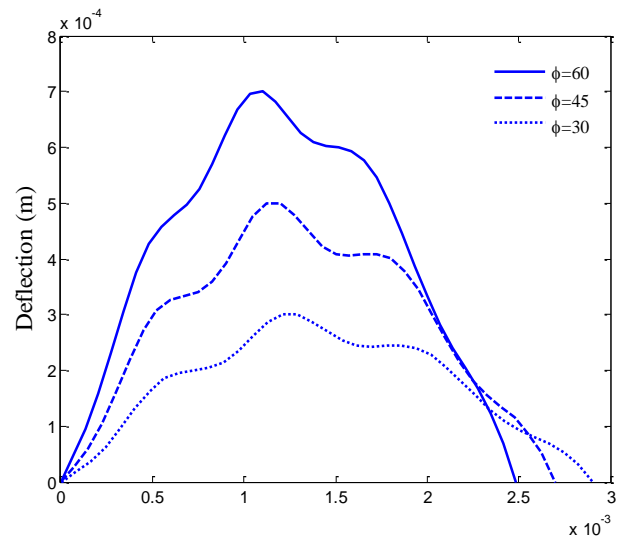


Fig. 13 The effect of core semi-vertex angle on the history of deflection

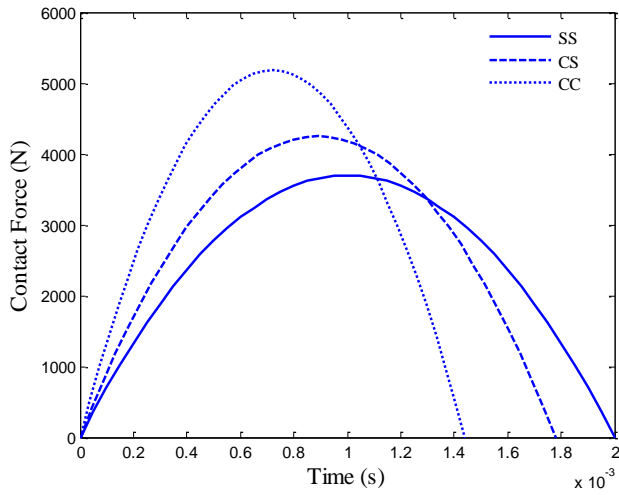


Fig. 14 The effect of boundary conditions on the history of contact force

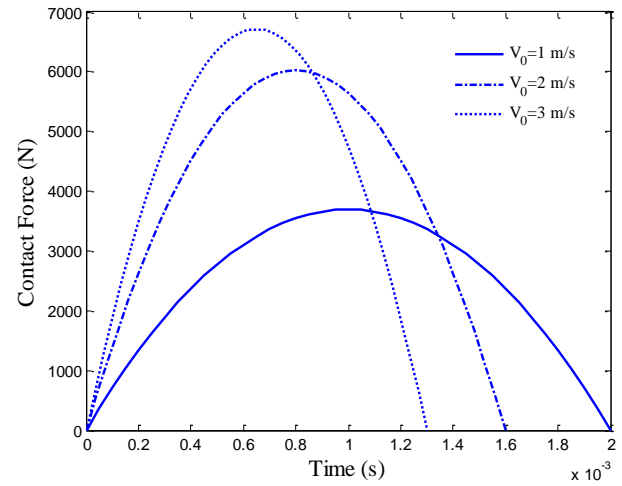


Fig. 16 The effect of impact velocity of impactor on the history of contact force

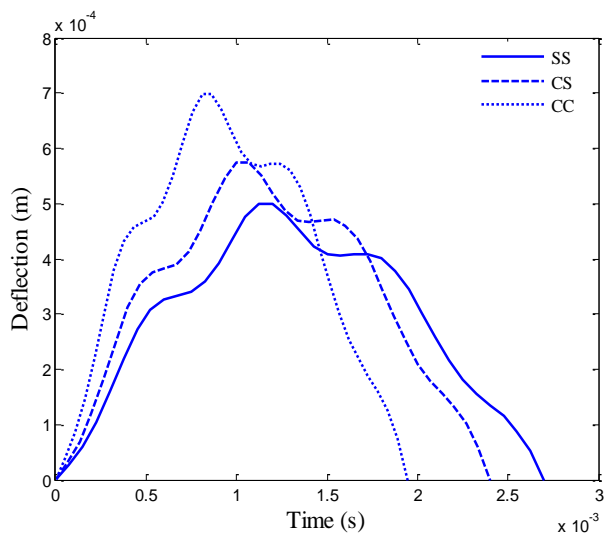


Fig. 15 The effect of boundary conditions on the history of deflection

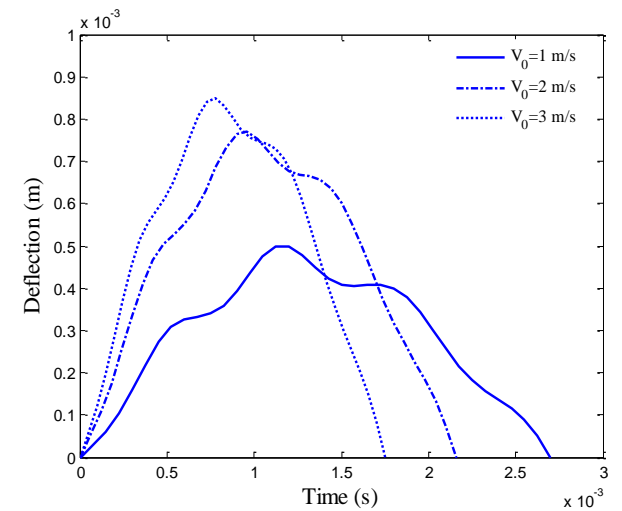


Fig. 17 The effect of impact velocity of impactor on the history of deflection

6.6 Boundary conditions effects

Figs. 14 and 15 show the effects of different boundary conditions on the contact force and deflection histories of structure, respectively. Four boundary conditions of simply-simply (SS), clamped-clamped (CC) and simply-clamped (SC) are considered. These figures show that considering CC boundary condition, the impact time decreases, while the maximum contact force increases slightly. Also, the central deflection of the top faces sheet increases considering CC boundary condition. It is due to the fact that the STCS with CC boundary condition has more rigidity with respect to other assumed boundary conditions.

6.7 Impact velocity effects

The impact velocity effect on the histories of contact force and deflection is demonstrated in Figs. 16 and 17, respectively. As can be seen the contact force and the

central deflection of the STCS increase with increasing impact velocity of impactor while the contact duration decreases as the impact velocity of impactor increases. The reason is that the higher impact velocity of impactor which accompanies higher impact energy, requires a larger deflection and accompanying contact force to dissipate it.

6.8 Structural damping effect

Figs. 18 and 19 illustrate the effect of structural damping on the histories of the contact force and dynamic deflection, respectively. It can be observed that with considering structural damping, the contact force and dynamic deflection decrees.

6.9 Dynamic stresses

Figs. 20-22 show the axial normal, circumferential normal and transverse stresses of the structure subjected to low-velocity impact for the top, bottom and core layers. The

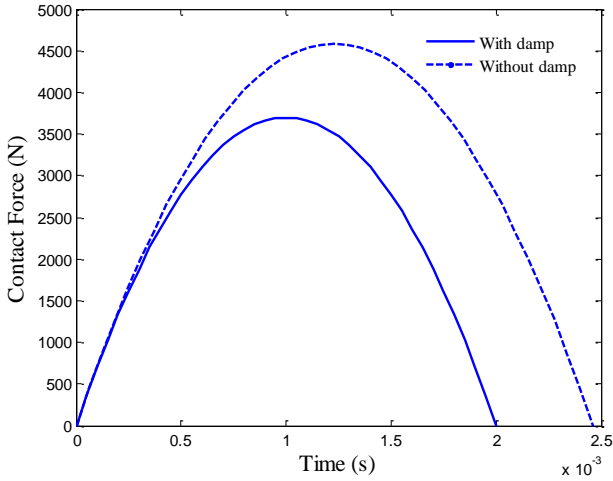


Fig. 18 The effect of structural damping on the history of contact force

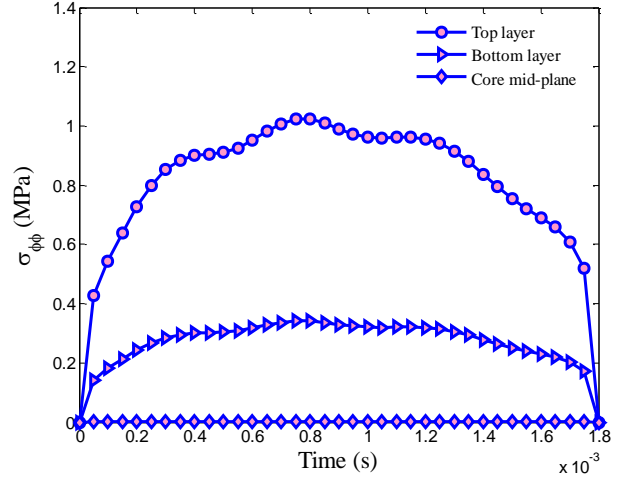


Fig. 21 Circumferential normal stress of the sandwich structure subjected to low-velocity impact

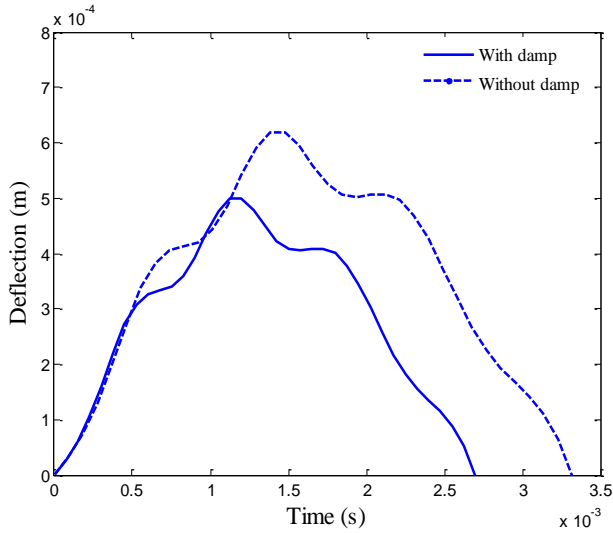


Fig. 19 The effect of the structural damping on the history of deflection

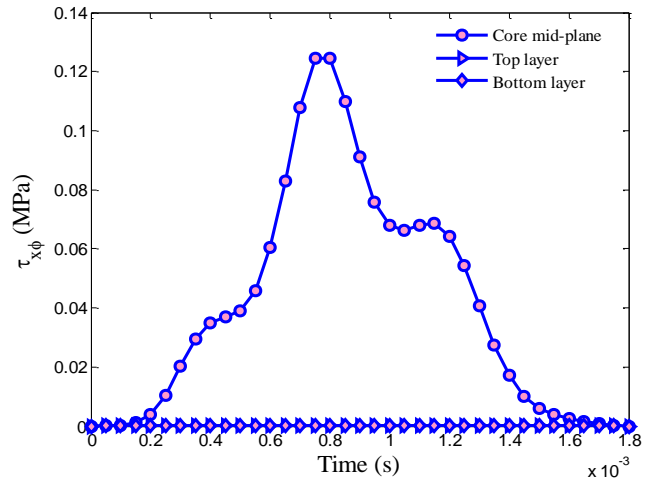


Fig. 22 Transverse stress of the sandwich structure subjected to low-velocity impact

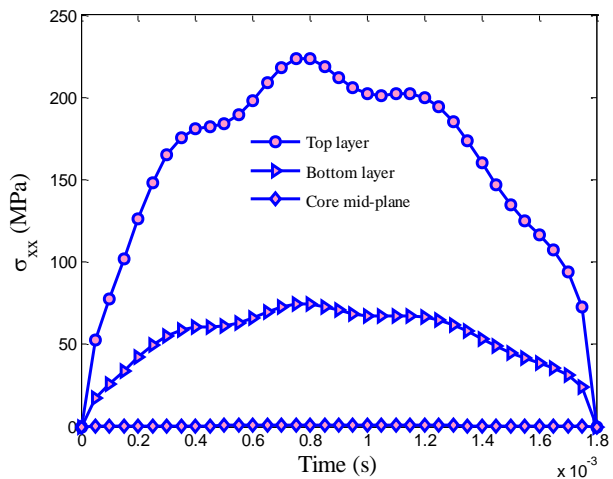


Fig. 20 Axial normal stress of the sandwich structure subjected to low-velocity impact

stress of the core is calculated for the neutral axis and the stresses of the top and bottom layers are shown for the face sheets. As can be seen, the normal stresses for the core layer and the transverse stress for the face sheets are zero. In addition, the normal stresses induced in top layer are higher than bottom layer since the top layer is subjected to impact load. Furthermore, the transverse stress in the core layer is maximum.

7. Conclusions

Low velocity impact response and dynamic stresses of orthotropic STCS with a soft/stiff flexible core was investigated applying a new equivalent TDOF spring-mass-damper model considering continuity boundary conditions. The face sheets are considered as laminated composite which follow the FSDT and the core is considered compressible (with transverse stress only) and incompressible (with in-plane and transverse stresses) based on high-order shear deformation theory of sandwich

structure. Using Hamilton's principal, the motion equations were derived and DQM was used for obtaining the contact force and deflection histories of structure. The effects of different parameters such as curvature of shell, in-plane stresses of core, layer number of face sheets, orientation angle of face sheets, cone semi vertex angle, boundary conditions and impact velocity of impactor were shown on low velocity impact response of STCS. Results indicated that:

- (1) Considering curvature and in-plane stresses of core effects increases the contact force and deflection of the sandwich structure while the contact duration decreases.
- (2) The maximum contact force and deflection of symmetric lamina were slightly greater than that of anti-symmetric one, while the contact duration for symmetric lamina was slightly less than that for the anti-symmetric one.
- (3) The maximum contact force and deflection of angle-ply are higher than cross-ply type.
- (4) The angle-ply lamina shortens slightly the contact .
- (5) It can be observed that with considering structural damping, the contact force and dynamic deflection decreases.
- (6) The contact force and the central deflection of the structure increases and the contact time decreases with increasing cone semi vertex angle.
- (7) Considering CC boundary condition, the impact time decreases, while the maximum contact force increases slightly.
- (8) The contact force and the central deflection of the STCS increase with increasing impact velocity of impactor while the contact duration decreases as the impact velocity of impactor increases.
- (9) In addition, the normal stresses induced in top layer are higher than bottom layer since the top layer is subjected to impact load.
- (10) The results of this study were validated as far as possible by other works.

Finally, it was hoped that the results of this paper would be beneficial for the design of low velocity impact response of sandwich structures used in aerospace and other industries.

References

- Abrate, S. (1991), "Impact on laminated composite materials", *Appl. Mech. Rev.*, **44**(4), 155-190.
- Abrate, S. (1997), "Localized impact on sandwich structures with laminated facings", *Appl. Mech. Rev.*, **50**(2), 69-82.
- Abrate, S. (2005), *Impact on Composite Structures*, Cambridge University Press.
- Allen, H.G. (2013), *Analysis and Design of Structural Sandwich Panels: The Commonwealth and International Library: Structures and Solid Body Mechanics Division*, Elsevier.
- Ambur, D.R. and Cruz, J. (1995), "Low-speed impact response characteristics of composite sandwich panels", *AIAA J.*, **95**, 1-14.
- Anderson, T.A. (2005), "An investigation of SDOF models for large mass impact on sandwich composites", *Compos. Part B: Eng.*, **36**(2), 135-142.
- Assarar, M., El Mahi, A. and Berthelot, J.M. (2009), "Damping analysis of sandwich composite materials", *J. Compos. Mat.*, **43**(13), 1461-1485.
- Bandyopadhyay, T., Karmakar, A. and Kishimoto, K. (2016), "Transient response of delaminated composite conical shells due to multiple low velocity impacts in hygrothermal environment", *Compos. Struct.*, **143**, 202-219.
- Bardell, N.S., Langley, R.S., Dunsdon, J.M. and Aglietti, G.S. (1999), "An h-p finite element vibration analysis of open conical sandwich panels and conical sandwich frusta", *J. Sound Vib.*, **226**(2), 345-377.
- Bellman, R. (Ed.), (1970), *Methods of Nonlinear Analysis*, Elsevier.
- Bhuiyan, M.A., Hosur, M.V. and Jeelani, S. (2009), "Low-velocity impact response of sandwich composites with nanophased foam core and biaxial ($\pm 45^\circ$) braided face sheets", *Compos. Part B: Eng.*, **40**(6), 561-571.
- Chai, G.B. and Zhu, S. (2011), "A review of low-velocity impact on sandwich structures", *Proceed. Institut. Mech. Eng., Part L: J. Mat. Des. Appl.*, **225**(4), 207-230.
- Cheng, X., Zhao, W., Liu, Sh., Xu, Y. and Bao, J. (2014), "Damage of scarf-repaired composite laminates subjected to low-velocity impacts", *Steel Compos. Struct., Int. J.*, **17**(2), 199-213.
- Dey, S. and Karmakar, A. (2014), "Time dependent response of low velocity impact induced composite conical shells under multiple delamination", *Mech. Time-Dep. Mat.*, **18**(1), 55-79.
- Dung, D.V., Hoa, L.K., Thuyet, B.T. and Nga, N.T. (2016), "Buckling analysis of functionally graded material (FGM) sandwich truncated conical shells reinforced by FGM stiffeners filled inside by elastic foundations", *Appl. Math. Mech.*, **37**(7), 879-902.
- Fatt, M.S.H. and Park, K.S. (2001), "Dynamic models for low-velocity impact damage of composite sandwich panels-Part A: Deformation", *Compos. Struct.*, **52**(3), 335-351.
- Feli, S., Khodadadian, S. and Safari, M. (2016), "A modified new analytical model for velocity impact response of circular composite sandwich panels", *J. Sandw. Struct. Mat.*, **18**(5), 552-578.
- Foo, C.C., Chai, G.B. and Seah, L.K. (2008), "A model to predict low-velocity impact response and damage in sandwich composites", *Compos. Sci. Tech.*, **68**(6), 1348-1356.
- Frostig, Y. and Thomsen, O.T. (2004), "High-order free vibration of sandwich panels with a flexible core", *Int. J. Solids Struct.*, **41**(5-6), 1697-1724.
- Garg, A.K., Khare, R.K. and Kant, T. (2006), "Higher-order closed-form solutions for free vibration of laminated composite and sandwich shells", *J. Sandw. Struct. Mat.*, **8**(3), 205-235.
- Ghorbanpour Arani, A., Kolahchi, R. and Zarei, M.Sh. (2015), "Visco-surface-nonlocal piezoelectricity effects on nonlinear dynamic stability of graphene sheets integrated with ZnO sensors and actuators using refined zigzag theory", *Compos. Struct.*, **132**, 506-526.
- Gong, S.W., Toh, S.L. and Shim, V.P.W. (1994), "The elastic response of orthotropic laminated cylindrical shells to low-velocity impact", *Compos. Eng.*, **4**(2), 247-266.
- Gong, S.W. and Lam, K.Y. (2000), "Effects of structural damping and stiffness on impact response of layered structure", *AIAA J.*, **38**(9), 1730-1735.
- Hassan, M.Z. and Cantwell, W.J. (2012), "The influence of core properties on the perforation resistance of sandwich structures-An experimental study", *Compos. Part B: Eng.*, **43**(8), 3231-3238.
- Hiel, C. and Ishai, O. (1992), "Design of highly damage-tolerant sandwich panels", *Proceedings of the 37th International SAMPE Symposium and Exhibition*, Anaheim, CA, USA,

- March, pp. 1228-1242.
- Hoo Fatt, M.S. and Park, K.S. (2001), "Dynamic models for low-velocity impact damage of composite sandwich panels—Part A: deformation", *J. Compos. Struct.*, **52**(3-4), 335-351.
- Horrigan, D.P.W., Aitken, R.R. and Moltschanivskyj, G. (2000), "Modelling of crushing due to impact in honeycomb sandwiches", *J. Sandw. Struct. Mat.*, **2**(2), 131-151.
- Khalili, M.R. (1992), "Analysis of the dynamic response of large orthotropic elastic plates to transverse impact and its application to fibre-reinforced plates", Doctoral Dissertation.
- Khalili, M.R., Malekzadeh, K. and Mittal, R.K. (2007), "Effect of physical and geometrical parameters on transverse low-velocity impact response of sandwich panels with a transversely flexible core", *Compos. Struct.*, **77**(4), 430-443.
- Khalili, S.M.R., Rahmani, O., MalekzadehFard, K. and Thomsen, O.T. (2014), "High-order modeling of circular cylindrical composite sandwich shells with a transversely compliant core subjected to low velocity impact", *Mech. Advanc. Mat. Struct.*, **21**(8), 680-695.
- Kheirikhah, M.M., Khalili, S.M.R. and Malekzadeh Fard, K. (2012), "Biaxial buckling analysis of soft-core composite sandwich plates using improved high-order theory", *Eur. J. Mech. A/Solids*, **31**(1), 54-66.
- Kolahchi, R. and Bidgoli, A.M. (2016), "Size-dependent sinusoidal beam model for dynamic instability of single-walled carbon nanotubes", *Appl. Math. Mech. -Engl. Ed.*, **37**(2), 265-274.
- Kolahchi, R., Safari, M. and Esmailpour, M. (2016), "Dynamic stability analysis of temperature-dependent functionally graded CNT-reinforced visco-plates resting on orthotropic elastomeric medium", *Compos. Struct.*, **150**, 255-265.
- Leijten, J., Bersee, H.E., Bergsma, O.K. and Beukers, A. (2009), "Experimental study of the low-velocity impact behaviour of primary sandwich structures in aircraft", *Compos. Part A: Appl. Sci. Manufact.*, **40**(2), 164-175.
- Malekzadeh, P. and Heydarpour, Y. (2013), "Free vibration analysis of rotating functionally graded truncated conical shells", *Compos. Struct.*, **97**, 176-188.
- Malekzadeh, K., Khalili, M.R. and Mittal, R.K. (2006), "Analytical prediction of low-velocity impact response of composite sandwich panels using new TDOF spring-mass-damper model", *J. Compos. Mat.*, **40**(18), 1671-1689.
- Malekzadeh, K., Khalili, M.R. and Mittal, R.K. (2007), "Response of composite sandwich panels with transversely flexible core to low-velocity transverse impact: A new dynamic model", *Int. J. Impact Eng.*, **34**(3), 522-543.
- Malekzadeh Fard, K.M. (2015), "Higher order static analysis of truncated conical sandwich panels with flexible cores", *Steel Compos. Struct.*, **19**(6), 1333-1354.
- Malekzadeh Fard, K.M. and Livani, M. (2015), "New enhanced higher order free vibration analysis of thick truncated conical sandwich shells with flexible cores", *Struct. Eng. Mech.*, **55**(4), 719-742.
- Manes, A., Gilioli, A., Sbarufatti, C. and Giglio, M. (2013), "Experimental and numerical investigations of low velocity impact on sandwich panels", *Compos. Struct.*, **99**, 8-18.
- Mittal, R.K. (1987), "A simplified analysis of the effect of transverse shear on the response of elastic plates to impact loading", *Int. J. Solids Struct.*, **23**(8), 1191-1203.
- Mittal, R.K. and Khalili, M.R. (1994), "Analysis of impact of a moving body on an orthotropic elastic plate", *AIAA J.*, **32**(4), 850-856.
- Morovat, F. (2016), "Analytical Solution for Buckling of Composite Sandwich Truncated Conical Shells subject to Combined External Pressure and Axial Compression Load", *Int. J. Advanc. Des. Manufact. Tech.*, **8**(4), 1-14.
- Nejad, M.Z., Jabbari, M. and Ghannad, M. (2015), "Elastic analysis of FGM rotating thick truncated conical shells with axially-varying properties under non-uniform pressure loading", *Compos. Struct.*, **122**, 561-569.
- Nettles, A.T. and Hodge, A.J. (1990), "Impact testing of glass/phenolic honeycomb panels with graphite/epoxy facesheets", *Proceedings of the 35th International SAMPE Symposium and Exhibition*, Anaheim, CA, USA, April.
- Noor, A.K., Burton, W.S. and Bert, C.W. (1996), "Computational models for sandwich panels and shells", *Appl. Mech. Rev.*, **49**(3), 155-199.
- Plantema, F.J. (1966), *Sandwich Construction: The Bending and Buckling of Sandwich Beams, Plates, and Shells*, Wiley.
- Reissner, E. (1953), "On a variational theorem for finite elastic deformations", *J. Math. Phys.*, **32**(2-3), 129-135.
- Setoodeh, A.R., Tahani, M. and Selahi, E. (2012), "Transient dynamic and free vibration analysis of functionally graded truncated conical shells with non-uniform thickness subjected to mechanical shock loading", *Compos. Part B: Eng.*, **43**(5), 2161-2171.
- Shivakumar, K.N., Elber, W. and Illg, W. (1985), "Prediction of impact force and duration due to low-velocity impact on circular composite laminates", *J. Appl. Mech.*, **52**(3), 674-680.
- Sofiyev, A.H. (2011), "Non-linear buckling behavior of FGM truncated conical shells subjected to axial load", *Int. J. Non-Linear Mech.*, **46**(5), 711-719.
- Sofiyev, A.H. (2014), "On the dynamic buckling of truncated conical shells with functionally graded coatings subject to a time dependent axial load in the large deformation", *Compos. Part B: Eng.*, **58**, 524-533.
- Struk, R. (1984), "Non-linear stability problem of an open conical sandwich shell under external pressure and compression", *Int. J. Non-linear Mech.*, **19**(3), 217-233.
- Sun, C.T. and Chattopadhyay, S. (1975), "Dynamic response of anisotropic laminated plates under initial stress to impact of a mass", *J. Appl. Mech.*, **42**(3), 693-698.
- Sun, C.T. and Juang, J.N. (1986), "Modeling global structural damping in trusses using simple continuum models", *AIAA J.*, **24**(1), 144-150.
- Sun, C. and Wu, C.L. (1991), "Low velocity impact of composite sandwich panels", *AIAA paper*, **91**, 1123-1129.
- Tang, M.Q. and Xu, J.C. (2013), "Nonlinear dynamic buckling for truncated sandwich shallow conical shell structure subjected to pulse impact", *Appl. Mech. Mat.*, **252**, 93-97.
- Tong, L. (1994), "Free vibration of laminated conical shells including transverse shear deformation", *Int. J. Solid Struct.*, **31**(4), 443-456.
- Tornabene, F. and Viola, E. (2009), "Free vibration analysis of functionally graded panels and shells of revolution", *Meccanica*, **44**(3), 255-281.
- Tornabene, F., Fantuzzi, N., Baccocchi, M. and Viola, E. (2015), "Higher-order theories for the free vibrations of doubly-curved laminated panels with curvilinear reinforcing fibers by means of a local version of the GDQ method", *Compos. Part B: Eng.*, **81**, 196-230.
- Vinson, J.R. (1999), *The Behavior of Sandwich Structures of Isotropic and Composite Materials*, CRC Press.
- Wang, J., Waas, A.M. and Wang, H. (2012), "Experimental Study on the Low-velocity Impact Behavior of Foam-core Sandwich Panels", *Proceedings of the 53rd AIAA/ASME/ASCE/ AHS/ASC Structures, Structural Dynamics and Materials Conference 20th AIAA/ASME/AHS Adaptive Structures Conference 14th AIAA*, p. 1701.
- Wang, J., Waas, A.M. and Wang, H. (2013), "Experimental and numerical study on the low-velocity impact behavior of foam-core sandwich panels", *Compos. Struct.*, **96**, 298-311.
- Wilkins, D.J., Bert, C.W. and Egle, D.M. (1970), "Free vibrations of orthotropic sandwich conical shells with various boundary

- conditions”, *J. Sound Vib.*, **13**(2), 211-228.
- Wu, H.Y.T. and Fu-Kuo, C. (1989), “Transient dynamic analysis of laminated composite plates subjected to transverse impact”, *Comput. Struct.*, **31**(3), 453-466.
- Zenkert, D. (1995), *An Introduction to Sandwich Construction*, Engineering Materials Advisory Services.
- Zhang, T., Yan, Y., Li, J. and Luo, H. (2016), “Low-velocity impact of honeycomb sandwich composite plates”, *J. Reinforc. Plast. Compos.*, **35**(1), 8-32.
- Zhou, D.W. and Stronge, W.J. (2006), “Low velocity impact denting of HSSA lightweight sandwich panel”, *Int. J. Mech. Sci.*, **48**(10), 1031-1045.

CC

$$[D_s^i] = \sum_L^{NL} \begin{bmatrix} Q_{55}H_0^3 & Q_{55}H_0^2 & Q_{56}H_0^3 & Q_{56}H_0^1 & Q_{55}H_1^2 & Q_{56}H_1^1 \\ & Q_{55}H_0^5 & Q_{56}H_0^2 & Q_{56}H_0^0 & Q_{55}H_1^5 & Q_{56}H_1^0 \\ & & Q_{66}H_0^3 & Q_{66}H_0^1 & Q_{65}H_1^2 & Q_{66}H_1^1 \\ & & & Q_{66}H_0^4 & Q_{65}H_1^0 & Q_{66}H_1^4 \\ & Sym. & & & Q_{55}H_2^5 & Q_{56}H_2^0 \\ & & & & & Q_{66}H_2^4 \end{bmatrix}^i \quad (A5)$$

that $i = t$ (top sheet), b (bottom sheet).

It is worth noting that $[B^i]$ matrices is similar to $[E^i]$ matrices and difference of $[A^i]$, $[B^i]$, $[E^i]$ and $[D^i]$ matrices are subscript “ j ” in “ H_j^i ” parameter in $[A^i]$ matrices is “ j ”, in $[B^i]$ and $[E^i]$ matrices is equal to “ $j + 1$ ” and in $[D^i]$ matrices is equal to “ $j + 2$ ”.